# Extrinsic Activin signaling cooperates with an intrinsic temporal program to increase mushroom body neuronal diversity

Anthony M. Rossi[1] and Claude Desplan[1]*

[1]Department of Biology, New York University, New York, NY 10003, USA.

*Lead contact

Correspondence: amr808@nyu.edu, cd38@nyu.edu

**Summary:**

Temporal patterning of neural progenitors leads to the sequential production of diverse neuronal types. To better understand how extrinsic cues interact with intrinsic temporal programs to contribute to temporal patterning, we studied the *Drosophila* mushroom body neural progenitors (neuroblasts). Each of these four neuroblasts divides ~250 times to sequentially produce only three main neuronal types over the course of ~9 days of development: γ, followed by α'β', and finally αβ neurons. The intrinsic temporal clock is composed of two RNA-binding proteins, IGF-II mRNA binding protein (Imp) and Syncrip (Syp), that are expressed in opposing temporal gradients. Activin signaling affects the production of α'β' neurons but whether and how this extrinsic cue interacts with the intrinsic temporal program was not known. We show that the Activin ligand Myoglianin produced from glia regulates the levels of the intrinsic temporal factor Imp in mushroom body neuroblasts. In neuroblasts mutant for the Activin signaling receptor *baboon*, Imp levels are higher than normal during the α'β' temporal window, leading to the specific loss of the α'β' neurons. The intrinsic temporal clock still progresses but with a delay, skipping the α'β' window without affecting the total number of neurons produced: The number of γ neurons increases, α'β' disappear and the number of αβ neurons decreases. Our results illustrate that an extrinsic cue modifies an intrinsic temporal program to increase neuronal diversity.

**Keywords:**

Temporal patterning, neuronal specification, intrinsic, extrinsic, *Drosophila*, mushroom body, Kenyon cells, RNA-binding, Activin, Myoglianin

## Introduction:

The building of intricate neural networks during development is controlled by highly coordinated patterning programs that regulate the generation of different neuronal types in the correct number, place and time. The sequential production of different neuronal types from individual progenitors, *i.e.* temporal patterning, is a conserved feature of neurogenesis (Cepko, 2014; Holguera and Desplan, 2018; Kohwi and Doe, 2013; Lodato and Arlotta, 2015). For instance, individual radial glia progenitors in the vertebrate cortex sequentially give rise to neurons that occupy the different cortical layers in an inside-out manner (Gao et al., 2014; Llorca et al., 2019). In *Drosophila*, neural progenitors (called neuroblasts) also give rise to different neuronal types sequentially. For example, projection neurons in the antennal lobe are born in a stereotyped temporal order and innervate specific glomeruli (Jefferis et al., 2001; Kao et al., 2012; Yu et al., 2010). In both of these examples, individual progenitors age concomitantly with the developing animal (e.g., from embryonic stages 11-17 in mouse and from the first larval stage (L1) to the end of the final larva stage (L3) in *Drosophila*). Thus, these progenitors are exposed to changing environments that could alter their neuronal output. Indeed, classic heterochronic transplantation experiments demonstrated that young cortical progenitors placed in an old host environment alter their output to match the host environment and produce upper-layer neurons (Desai and McConnell, 2000; McConnell, 1988; McConnell and Kaznowski, 1991).

The adult *Drosophila* central brain is built from ~100 neuroblasts (Lee et al., 2020; Urbach and Technau, 2004; Wong et al., 2013; Yu et al., 2013a) that divide continuously from L1 to L3 (Homem et al., 2014; Sousa-Nunes et al., 2010; Yang et al., 2017). Each asymmetric division regenerates the neuroblast and produces an intermediate progenitor called ganglion mother cell (GMC) that divides only once, typically producing two different cell types (Lin et al., 2010; Spana and Doe, 1996; Truman et al.,

2010). Thus, during larval life central brain neuroblasts divide 50-60 times, sequentially producing many different neuronal types. All central brain neuroblasts progress through opposing temporal gradients of two RNA-binding proteins as they age: IGF-II mRNA binding protein (Imp) when they are young and Syncrip (Syp) when they are old (Liu et al., 2015; Syed et al., 2017b, 2017a; Yang et al., 2015). Loss of Imp or Syp in antennal lobe or Type II neuroblasts affects the ratio of young to old neuronal types (Liu et al., 2015; Ren et al., 2017). Imp and Syp also affect neuroblast lifespan (Yang et al., 2017). Thus, a single temporal program can affect both the diversity of neuronal types produced and their numbers.

Since central brain neuroblasts produce different neuronal types through developmental time, roles for extrinsic cues have recently garnered attention. Ecdysone triggers all the major developmental transitions including progression into the different larval stages and entry in pupation (Yamanaka et al., 2013). The majority of central brain neuroblasts are not responsive to ecdysone until mid-larval life when they begin to express the Ecdysone Receptor (EcR) (Syed et al., 2017a). Expressing a dominant-negative version of EcR (EcR-DN) in Type II neuroblasts delays the Imp to Syp transition that normally occurs ~60 hours after larval hatching (ALH). This leads to many more cells that express the early-born marker gene Repo and fewer cells that express the late-born marker gene Bsh.

To further understand how extrinsic signals contribute to temporal patterning, we studied mushroom body neuroblasts because of the deep understanding of their development. The mushroom body is comprised of ~2,000 neurons (Kenyon cells) that belong to only three main neuronal types that have unique morphologies and play distinct roles in learning and memory (Cognigni et al., 2018; Ito et al., 1997; Lee et al., 1999). They receive input mainly from ~200 projection neurons that each relays odor information from olfactory receptor neurons (Vosshall and Stocker, 2007). Each projection neuron connects to a random subset of Kenyon cells and each Kenyon cell receives input from ~7 different projection neurons (Jefferis et al., 2007; Murthy et al., 2008; Turner et al., 2008). This connectivity pattern requires a large number of mushroom body neurons (~2,000) to represent complex odors (Hige, 2018). To produce this very large number of neurons, mushroom body development is unique in many respects. Mushroom body neurons are born from four identical neuroblasts that divide continuously

(unlike any other neuroblast) from the late embryonic stages until the end of pupation (~9 days for ~250 divisions each) (Fig. 1A) (Ito et al., 1997; Kraft et al., 2016; Kunz et al., 2012; Kurusu et al., 2009; Lee et al., 1999; Pahl et al., 2019; Siegrist et al., 2010; Sipe and Siegrist, 2017). Furthermore, the two neurons born from each mushroom body GMC are identical. The neuronal simplicity of the adult mushroom body makes it ideal to study how extrinsic cues might affect diversity since the loss of any single neuronal type is obvious given that each is represented hundreds of times.

The three main neuronal types that make up the adult mushroom body are produced sequentially during neurogenesis: first γ, followed by α'β', and then αβ neurons (Lee et al., 1999) (Fig. 1A), representing the simplest lineage in the central brain. The γ temporal window extends from L1 (the first larval stage) until mid L3 (the final larval stage) when animals attain critical weight and are committed to metamorphosis; the α'β' window from mid L3 to the beginning of pupation, and the αβ window from pupation until eclosion (the end of development). Like all other central brain neuroblasts Imp and Syp are expressed by mushroom body neuroblasts, but in much shallower gradients through time, which accounts for their extended lifespan (Liu et al., 2015; Yang et al., 2017). Imp and Syp are inherited by newborn neurons where they instruct temporal identity. Imp positively and Syp negatively regulate the translation of *chronologically inappropriate morphogenesis* (*chinmo*), a gene encoding a transcription factor that acts as a temporal morphogen in neurons (Kao et al., 2012; Ren et al., 2017; Zhu et al., 2006). The first-born γ neurons are produced for the first ~85 cell divisions, when Imp levels in neuroblasts, and thus Chinmo in neurons, are high. α'β' neurons are produced for the next ~40 divisions, when Imp and Syp are at similar low levels that translate into lower Chinmo levels in neurons. Low Chinmo then regulates the expression in neurons of *maternal gene required for meiosis* (*mamo*), which encodes a transcription factor that specifies the α'β' fate and whose mRNA is stabilized by Syp (Liu et al., 2019). αβ neurons are generated for the final ~125 neuroblast divisions, when Syp levels are high, Imp is absent in neuroblasts, and thus Chinmo and Mamo are no longer expressed in neurons.

Extrinsic cues are known to have important roles in regulating neuronal specification and differentiation during mushroom body neurogenesis. The ecdysone peak that controls entry into pupation regulates γ neuron axonal remodeling (Lee et al., 2000). Ecdysone was also proposed to be required for the final differentiation of α'β' neurons (Marchetti and Tavosanis, 2017). EcR expression in γ neurons is timed by Activin signaling, a member of the TGFβ family, from local glia (Awasaki et al., 2011; Zheng et al., 2003). Activin signaling is also required for α'β' specification (Marchetti and Tavosanis, 2019): Knocking-down the Activin pathway receptor Baboon (Babo) leads to the loss of α'β' neurons. It was proposed that Activin signaling in mushroom body neuroblasts regulates the expression of EcR in prospective α'β' neurons, providing a link between the two signaling pathways (Marchetti and Tavosanis, 2019).

Although there is strong evidence that extrinsic cues have important functions in neuronal patterning in the *Drosophila* central brain, it remains unknown how extrinsic temporal cues interface with the Imp and Syp intrinsic temporal program to regulate neuronal specification. Here we address this question using the developing mushroom bodies. We independently discovered that Activin signaling from glia is required for α'β' specification. However, we show that Activin signaling lowers the levels of the intrinsic factor Imp in mushroom body neuroblasts to define the mid α'β' temporal identity window. Removing the Activin receptor Babo in mutant clones leads to the loss of α'β' neurons, to fewer last-born αβ neurons, and to the generation of additional first-born γ neurons without affecting overall clone size. This appears to be caused by a delayed decrease in Imp levels, although the intrinsic temporal clock still progresses even in the absence of Activin signaling. We also demonstrate that ecdysone signaling is not necessary for the specification of α'β' neurons, although it might still be involved in later α'β' differentiation. Our results provide a model for how intrinsic and extrinsic temporal programs operate within individual progenitors to regulate neuronal specification.

**Results:**

**α'β' neurons are not generated from *babo* mutant neuroblasts**

The production of the three different mushroom body neuronal types occurs within specific developmental stages of larval and pupal development. That is, the γ window extends from L1 to mid L3, the α'β' window from mid L3 to pupation, and the αβ window from pupation to eclosion (Fig. 1A) (Lee et al., 1999). This means that extrinsic cues could play a role in controlling or fine-tuning transitions between these temporal windows. Additionally, the specification of neuronal identity within each temporal window could be aided by extrinsic cues. To test these hypotheses, we used Mosaic Analysis with Repressible Cell Marker (MARCM) (Lee and Luo, 1999) to test the function of receptors for inter-cellular signaling pathways with known roles either in mushroom body neurogenesis (Activin and Ecdysone) (Lee et al., 2000; Marchetti and Tavosanis, 2017, 2019; Zheng et al., 2003) or more broadly during nervous system development (Hedgehog and juvenile hormone) (Fig. S1) (Baumann et al., 2017; Chai et al., 2013). We induced mushroom body neuroblast clones at L1 and compared the axonal morphologies of adult neurons born from mutant neuroblasts to neurons born from surrounding wildtype neuroblasts. To identify mushroom body axonal lobes (both mutant and wildtype), we used antibodies to the Rho guanine exchange factor Trio (a weak γ and strong α'β' cytoplasmic marker ) and to the cell adhesion molecule Fasciclin II (FasII) (an axonal γ and αβ marker) (Fig. 1B) (Awasaki et al., 2000; Crittenden et al., 1998). To visualize mushroom body neurons within clones we expressed *UAS-CD8::GFP* under the control of *OK107-Gal4* (referred to as *mb-Gal4* hereafter), a *Gal4* enhancer trap in *eyeless* and a common mushroom body *Gal4* driver that strongly labels all mushroom body neuronal types during development and in the adult, and weakly mushroom body neuroblasts and young neurons throughout development (Connolly et al., 1996; Liu et al., 2015; Zhu et al., 2006).

In wildtype clones induced at L1, $GFP^+$ axons projected to all five mushroom body lobes: α, α′, β, β' (hidden behind the γ lobe in max projections), and γ (Fig. 1D, Fig. S1A). In clones mutant for *babo*, we did not detect $GFP^+$ axons within the α'β' lobes, which remained visible by Trio staining due to the presence of wildtype α'β' neurons (Fig. 1E, Fig. S1B). In addition, and as previously described, γ neurons

within *babo* mutant clones remained unpruned (visualized by vertical GFP$^+$ axons that were Trio$^+$ and FasII$^+$), providing a positive control since γ remodeling is known to require Activin signaling (Fig. 1E, S1B) (Awasaki et al., 2011; Yu et al., 2013b; Zheng et al., 2003).

Babo is the sole Type I receptor in the Activin pathway (a member of the TGFβ family of signaling molecules). Babo with its Type II co-receptors binds four different Activin ligands and acts through the transcription factor Smad on X (Smad2) (Brummel et al., 1999; Upadhyay et al., 2017). We induced *Smad2* mutant clones at L1 and characterized adult axonal morphologies. Similar to *babo* mutant clones, *Smad2* clones were missing α'β' neurons and also contained unpruned γ neurons (Fig. S1I).

The absence of GFP$^+$ axons within the α'β' lobes in *babo* mutant clones could be due to the loss of axonal projections, or to the loss of neuronal identity. Using antibodies against Trio and Mamo that strongly label α'β' neuron cell bodies in the adult (Fig. 1B, Fig. S1J) (Alyagor et al., 2018; Awasaki et al., 2000; Croset et al., 2018; Liu et al., 2019), we detected strong Trio$^+$ and Mamo$^+$ cells within adult GFP$^+$ clones induced at L1 (Fig. 1F, Fig. S1K). In *babo* mutant clones however, the vast majority of strong Trio$^+$ and Mamo$^+$ cells inside clones were missing compared to surrounding wildtype neurons (Fig. 1G, Fig. S1L), suggesting that α'β' neurons were not specified. We quantified the number of α'β' neurons in wildtype and *babo* clones by counting the number of strong Mamo$^+$ cells within a clone versus the total number of strong Mamo$^+$ cells outside the clone. In wildtype MARCM clones affecting a single mushroom body neuroblast (n=7), the percentage of all α'β' neurons that were present within the clones was 25.5%, the expected ratio since each mushroom body is built from four identical neuroblasts (Fig. 1H) (Ito et al., 1997; Lee et al., 1999). In comparison, in *babo* mutant clones (n=8) the percentage of α'β' neurons within clones was 2.2% (Fig. 1H). These data suggest that Activin signaling is necessary for α'β' specification.

We next sought to determine the fate of the missing α'β' neurons in *babo* clones, particularly since there was no significant difference in average clone sizes between mutant and control clones labeled with *mb-Gal4* (wildtype: clone size= 533.6, n=7; *babo*: clone size = 551.3, n=7) (Fig. 1H'), which

suggests that there is no defect in neuroblast proliferation, and that α'β' neurons are not lost by cell death in *babo* clones. However, to directly test whether cell death played a role, we expressed the caspase inhibitor P35 in *babo* mutant clones (Fig. S2A). However, α'β' neurons were still missing in the adult (Fig. S2A), indicating that α'β' neurons are not generated and then die. We thus tested whether the γ or αβ temporal windows were extended in *babo* mutant clones. We made MARCM clones in which the γ, α'β' or αβ neurons were specifically marked with different *Gal4* lines, and then quantified the total number of $GFP^+$ neurons in wildtype versus *babo* mutant clones (Fig. 1I-K, Fig. S2B-M). Using *R71G10-Gal4* (Issman-Zecharya and Schuldiner, 2014) (referred to as *γ-Gal4*), the average number of γ neurons trended higher in *babo* mutant clones, although not significantly (wildtype: 154.3, n=10; *babo*: 178.4, n=12) (Fig. 1I, Fig. S2B-E), likely because the number of γ neurons directly depends on the time of clone induction. α'β' neurons, marked by *41C07-Gal4* (referred to as *α'β'-Gal4*), were mostly missing in *babo* mutant clones compared to wildtype clones (wildtype: 81.5, n=4; *babo*: 2.1, n=8,) consistent with our previous results when counting strong $Mamo^+$ cells in *babo* clones marked by *mb-Gal4* (Fig. 1H, 1J, Fig. S2F-I). The average number of αβ neurons, marked by *44E04-Gal4* (referred to as *αβ-Gal4*), was significantly reduced in *babo* versus wildtype clones (wildtype: 276, n=7,; *babo*: 228.9, n=8) (Fig. 1K, Fig. S2J-M). Together, these results suggest that additional γ neurons are produced, and that fewer αβ neurons are generated, in *babo* mutant clones. We note that the total number of neurons labeled by our neuron type specific *Gal4* drivers did not add up to the expected number of ~500 neurons in *babo* mutant clones, which is likely explained by the large variability in the number of γ neurons labeled by *γ-Gal4* in *babo* mutant clones. These results are consistent with a recent report showing the loss of α'β' neurons in the adult following knockdown of *babo* with RNA interference (RNAi), which was explained by a role in regulating EcR expression in neurons (see below) (Marchetti and Tavosanis, 2019). Here, we focused on understanding whether and how Activin signaling interacts with the intrinsic Imp and Syp temporal program.

**Activin signaling acts in neuroblasts to lower Imp levels and specify α'β' neurons**

Given that α'β' neuronal specification is intrinsically controlled by Imp and Syp (Liu et al., 2015), we asked whether Activin signaling acts through or in parallel to this intrinsic temporal system, specifically at L3 when α'β' neurons are being produced. We first asked whether *babo* is expressed at L3 in mushroom body neuroblasts. Based on published transcriptome data collected from mushroom body neuroblasts at different developmental stages (Liu et al., 2015; Yang et al., 2015), *babo* is expressed evenly through time in mushroom body neuroblasts, unlike the two RNA binding proteins *Imp* and *Syp* (Fig. S3A). Although this measure does not take into account the possibility of post-transcriptional regulation, it is likely that the Activin signaling pathway is temporally controlled by ligand interaction and not by differential expression of *babo*.

To directly test whether Activin signaling acts on Imp and Syp to affect α'β' specification, we induced MARCM clones for *babo* at L1 and compared the Imp to Syp protein ratio in mutant mushroom body neuroblasts to surrounding wildtype neuroblasts at wandering L3 (Fig. 2). The average Imp to Syp ratio was significantly higher in *babo* neuroblasts (ratio: 4.2; n=9 from 4 different brains) compared to wildtype neuroblasts (ratio: 2.4; n=23 from the same 4 brains as *babo*) at L3, driven by a significantly higher Imp level in mutant neuroblasts (Fig. 2, Fig. S3B) while Syp was not significantly different (Fig. SB'). In addition, the α'β' neuronal marker Mamo (Liu et al., 2019) was lost in *babo* mutant clones at L3 (Fig. S3C), consistent with the notion that high Imp levels block α'β' specification. The significantly higher Imp to Syp ratio in *babo* mutant neuroblasts persisted even ~24 hours After Pupal Formation (APF) (*babo* ratio: 0.58; n=7 from 6 different brains; wildtype ratio: 0.27; n=27 from the same 6 brains as *babo*), once again driven by higher Imp levels (Fig. S3D-I). Together, these results indicate that Activin signaling lowers Imp levels at late larval and early pupal stages. Importantly, although Imp was higher in

*babo* mutant neuroblasts and persisted longer, the absolute level of Imp still decreased significantly albeit with prolonged kinetics, while the absolute level of Syp was higher in *babo* mutant neuroblasts at ~24 hours APF vs. L3 (Fig. S3J-J'): Thus, these changes are either intrinsically regulated or are affected by additional extrinsic factors. Our finding that Imp was higher in *babo* mutant neuroblasts at L3 is also consistent with our suggestion that additional γ neurons are produced and that the number of αβ neurons decreases, since higher Imp levels for a longer period of time may lead to the production of γ neurons during the α'β' time window and expanding to the beginning of the αβ window. The lack of α'β' neurons in *babo* mutant clones even though Imp levels were finally low at ~24 hours APF suggests that α'β' specification can only occur from L3 to the start of pupation.

We have shown that Activin signaling functions in mushroom body neuroblasts to decrease Imp during L3. However, previous studies have shown that Babo also acts post-mitotically in mushroom body γ neurons where it times the expression of EcR for their remodeling, indicating that Babo can act independently in neuroblasts and in neurons (Zheng et al., 2003). To test if Activin signaling functions post-mitotically in prospective α'β' neurons, we characterized the morphology of *babo* mutant neurons born from ganglion mother cell (GMC) clones induced during mid-late L3, the time at which α'β' neurons are born. GMCs are intermediate progenitors that divide only once to produce two neurons. In this way, the role of Babo in prospective α'β' neurons can be tested without affecting mushroom body neuroblasts: α'β' neurons were present in *babo* GMC clones (n=34/34), observable by axonal projections into the Trio labeled α'β' lobes (Fig. S3K-K'). As a positive control for the efficiency of *babo* GMC clones, we also made *babo* GMC clones at L1 to target γ neurons. In the majority of cases, γ axons remained unpruned (n=8/10, Fig. S3L-L') (Zheng et al., 2003). These results show that Activin signaling acts in mushroom body neuroblasts, and not in neurons, to specify the α'β' fate.

**Activin signaling is sufficient to expand production of α'β' neurons**

Since Activin signaling functions in mushroom body neuroblasts and is necessary for α'β' specification, we next investigated whether it is sufficient for the α'β' fate. We expressed a constitutively active form of the Babo receptor (*UAS-Babo-Act*) throughout development in MARCM clones with *mb-Gal4* and assessed the total number of α'β' neurons in the adult by strong Mamo expression. While in wildtype clones the percentage of α'β' neurons was 25.5% (n=7), the number of α'β' neurons present within *UAS-Babo-Act* clones significantly increased to 32% (n=4) (Fig. 3A-B). To ask when these additional α'β' neurons were produced, we characterized the expression of the α'β' marker Mamo in young neurons at early L3, when γ neurons are being produced. In comparison to wildtype neurons, Mamo was expressed in neurons in *UAS-Babo-Act* clones at this stage (Fig. 3C-D). These results confirm the precocious specification of α'β' neurons, although constitutively expressing an activated version of Babo did not result in adult clones consisting entirely of α'β' neurons.

**Glia are the source of the Activin ligand Myoglianin to specify α'β' neurons**

Our finding that Activin signaling plays an important role in specifying α'β' identity during mushroom body development led us to question from where the Activin ligand originates. Glia secrete the Activin ligand Myoglianin (Myo) to initiate γ neuron remodeling by activating EcR at L3 (Awasaki et al., 2011; Yu et al., 2013b). Therefore, we hypothesized that Myo from glia may also regulate α'β' specification. To test this, we knocked-down *myo* by expressing *UAS-myo-RNAi* with *repo-Gal4*, a driver expressed in all glia, and quantified the total number of α'β' neurons based on strong Mamo expression in the adult (Fig. 4A-E). In comparison to control (428.9, n=10), the number of α'β' neurons was dramatically reduced (106.6; n=10) (Fig. 4E). Mamo was also not expressed in mushroom body neurons at L3 (Fig. 4F-G). Importantly, EcR was not expressed in γ neurons at this stage, providing a positive control for the efficiency of *UAS-myo-RNAi*. We note that even though the number of α'β' neurons was reduced in this experiment, *myo* knockdown was weaker than *babo* mutant clones, possibly due to incomplete

knockdown of *myo* or because more than one ligand (or more than one source) contribute to α'β' specification. Our results are consistent with a recent report that also showed that glia are the source of Myo for α'β' specification (Marchetti and Tavosanis, 2019).

**α'β' neurons are specified by low Imp levels at L3**

We and others have shown that Activin signaling is necessary for α'β' specification (Marchetti and Tavosanis, 2019). We have shown that Activin signaling acts by lowering Imp levels at L3. Although Imp is required for α'β' specification (Fig. S4A-C) (Liu et al., 2015), we wanted to determine whether low Imp levels are required at L3. We therefore characterized Mamo expression in young neurons at L3 following knockdown (*UAS-Imp-RNAi*) or overexpression (*UAS-Imp-OE*) of *Imp* with *mb-Gal4*. (Fig. 5A-C) (Liu et al., 2015). Consistent with our model, Mamo was not expressed in either condition. Although knocking-down *Syp* by expressing *UAS-Syp-RNAi* led to the loss of Mamo, its early overexpression (*UAS-Syp-OE*) did not (Fig. 5D-E). The loss of Mamo in *Syp* knockdown is consistent with its role in stabilizing *mamo* transcripts at L3 (Liu et al., 2019). We conclude that low Imp and low or high Syp levels are required for α'β' specification. Consistent with this, we were unable to rescue the loss of α'β' neurons in *babo* mutant clones by constitutively repressing Imp with *UAS-Imp-RNAi* (0.2%, n=7) (Fig. S4I, S4N, S4P), likely due Imp reduction below the threshold required for α'β' specification. However, we could rescue *babo* mutant clones by expressing *UAS-babo* (21.1%, n=6) (Fig. S4A-C, S4K-M, S4P). Overexpressing Syp (*UAS-Syp-OE*) to reduce the altered Imp:Syp ratio in *babo* mutant clones also did not rescue α'β' neurons (1.8%, n=7) (Fig. S4J, S4O-P), further highlighting that Imp but not Syp levels are important for α'β' specification.

**Ecdysone signaling is not be necessary for α'β' specification**

It has been proposed that Activin signaling in mushroom body neuroblasts leads to EcR expression in neurons and that ecdysone signaling at late L3 induces differentiation of α'β' neurons (Marchetti and Tavosanis, 2017, 2019). The role of ecdysone was tested by expressing a dominant-negative ecdysone

receptor (*UAS-EcR-DN*). We confirmed these results by also expressing *UAS-EcR-DN* driven by *mb-Gal4* and were unable to detect $GFP^+$ mutant axons within adult α'β' lobes marked by Trio (Fig. 6A-B). In addition, strong $Trio^+$ and $Mamo^+$ cells were missing inside *UAS-EcR-DN* mutant clones compared to wildtype clones (wildtype: 25.5%, n=7; *UAS-EcR-DN*: 3.4%, n=6) (Fig. 6C-E, Fig. S5A). However, we were surprised to find that α'β' neurons were still present in mutant clones for the EcR co-receptor *ultraspiracle* (*usp*) (Fig. 6F). Therefore, we sought to better understand the function of EcR-DN. Unlike our result in *babo* mutant neuroblasts, we did not observe a significant difference in the average Imp to Syp protein ratio at L3 in *UAS-EcR-DN* expressing mushroom body neuroblasts with *mb-Gal4* (*UAS-EcR-DN* ratio: 2.6, n=4 from 4 different brains; wildtype ratio: 1.7, n=27 from the same 4 brains as *UAS-EcR-DN*) (Fig. 6G-J, S5B-B'). In order to specify α'β' neurons, EcR should function in neuroblasts at the time these neurons are produced. However, driving strong expression of *UAS-EcR-DN* in neuroblast with *inscuteable-Gal4* (referred to as *NB-Gal4*) and labeling all adult neurons with *R13F02-Gal4* (referred to as *mb2-Gal4*) (Jenett et al., 2012) did not lead to the loss of α'β' neurons in the adult (Fig. 6K-N, S5C-D). These results indicate that EcR-DN acts in neurons, not neuroblasts, to lead to the loss of α'β' neurons**,** which is consistent with our inability to detect EcR protein in mushroom body neuroblasts at wandering L3 (Fig. S5E-E), although EcR was expressed in γ neurons at this stage (Fig. S5F-F') (Lee et al., 2000; Liu et al., 2015; Marchetti and Tavosanis, 2017).

Since Mamo expression marks α'β' neurons during development (Liu et al., 2019), we asked whether EcR-DN affects Mamo expression. At L3, Mamo expression was lost in *UAS-EcR-DN* expressing clones driven by *mb-Gal4* (Fig. 6P) but it was not affected by expression of *UAS-EcR-RNAi* (Fig. 6Q) although the RNAi was effective since we could not detect EcR protein in mushroom body neurons (Fig. 6O, 6Q). Given these contradictory results, we compared Mamo and EcR expression at L3: Mamo and EcR appeared mutually exclusive as EcR was not expressed in young α'β' neurons (see Fig. 6O''). These results are also consistent with our inability to rescue the loss of α'β' neurons in *babo* mutant clones by expressing *UAS-EcR* (Fig. S5G-H). In summary, α'β' neurons were only lost in adult

clones when expressing *UAS-EcR-DN* and not in *usp* mutant clones and α'β' neurons were still present in *EcR-RNAi* in L3. In addition, EcR protein was not detected in Mamo$^{+}$ cells during development, although expressing *UAS-EcR-DN* blocked Mamo expression at L3. We conclude that ecdysone signaling is not involved in α'β' specification although it might still be required for late differentiation of α'β' neurons (Marchetti and Tavosanis, 2017). We therefore speculate that loss of α'β' neurons with *UAS-EcR-DN* is caused by off-target inhibition of Mamo.

## Discussion:

### Establishment of mushroom body neuronal identities

Mushroom body neurogenesis is unique and programmed to generate many copies of a few neuronal types.

During the early stages of mushroom body development, high Imp levels are translated into high Chinmo levels to specify γ identity. As in other central brain neuroblasts, as development proceeds, inhibitory interactions between Imp and Syp help create a slow decrease of Imp and a corresponding increase of Syp. However, at the end of the γ temporal window (mid L3), Activin signaling from glia acts to rapidly reduce Imp levels without significantly affecting Syp, establishing a period of low Imp (and thus low Chinmo) and also low Syp. This is required for activating effector genes in prospective α'β' neurons, including Mamo, whose translation is promoted by Syp (Liu et al., 2019). The production of αβ identity begins when Imp (and thus Chinmo) are further decreased and Syp levels are high (modeled in Fig. 7). The peak of ecdysone that instructs the larval to pupal transitions instructs γ neurons to remodel (Zheng et al., 2003) but is not involved in the specification of α'β' identity, although it might still play a role in their final fate (Marchetti and Tavosanis, 2017). Ecdysone signaling in αβ neurons is also involved in quickly lowering Chinmo levels (Kucherenko et al., 2012; Wu et al., 2012).

In this study, we have focused on the three main classes of mushroom body neurons although at least 7 subtypes exist: 2 γ, 2 α'β' and 3 αβ (Aso et al., 2014; Shih et al., 2019). The subtypes are specified

sequentially (Aso et al., 2014) suggesting that each of the three broad mushroom body temporal windows can be subdivided further, either by fine-scale reading of the changing Imp and Syp gradients, by additional extrinsic cues, or perhaps by a tTF series as in other neuroblasts.

**Temporal patterning of *Drosophila* central brain neuroblasts**

Postembryonic central brain neuroblasts are long-lived and divide on average ~50 times. Unlike in other regions of the developing *Drosophila* brain, rapidly progressing series of tTFs have not yet been described in these neuroblasts (Doe, 2017; Holguera and Desplan, 2018; Kohwi and Doe, 2013; Rossi et al., 2017). Instead, they express Imp and Syp in opposing temporal gradients (Liu et al., 2015; Ren et al., 2017; Syed et al., 2017a). Conceptually, how Imp and Syp gradients translate into different neuronal identities through time has been compared to how morphogen gradients pattern tissues in space (Liu et al., 2019, 2015). During patterning of the anterior-posterior axis of the *Drosophila* embryo, the anterior gradient of the Bicoid morphogen and the posterior Nanos gradient are converted into discrete spatial domains that define cell fates (Briscoe and Small, 2015; Liu et al., 2019). Since gradients contain unlimited information, differences in Imp and Syp levels through time could translate into different neuronal types. Another intriguing possibility is that tTF series could act downstream of Imp and Syp, similarly to how the gap genes in the *Drosophila* embryo act downstream of the anterior-posterior morphogens. We have shown that another possibility is that temporal extrinsic cues can be incorporated by individual progenitors to increase neuronal diversity. In mushroom body neuroblasts Activin signaling acts directly on the intrinsic program, effectively converting two broad temporal windows into three to help define an additional neuronal type. We propose that subdividing the broad Imp and Syp temporal windows by extrinsic cues may be a simple way to increase neuronal diversity in other central brain neuroblasts.

We have also shown that Activin signaling times the Imp to Syp transition for mushroom body neuroblasts, similar to the function of ecdysone for other central brain neuroblasts (Syed et al., 2017a). In

both cases however, the switch still occurs, indicating that a separate independent clock continues to tick. This role for extrinsic cues during *Drosophila* neurogenesis is reminiscent of their roles on individual vertebrate progenitors. For example, hindbrain neural stem cells progressively produce motor neurons followed by serotonergic neurons before switching to producing glia (Chleilat et al., 2018; Dias et al., 2014). The motor neuron to serotonergic neuron switch is fine-tuned by TGFβ signaling. It would be interesting to determine if hindbrain neuronal subtypes are lost in TGFβ mutants, similar to how α'β' identity is lost in the mushroom bodies in *babo* mutants.

**Ecdysone signaling is not necessary for α'β' specification**

EcR is temporally expressed in mushroom body neurons at late L3. At this stage, both γ and α'β' neurons exist and new α'β' neurons are still being generated. The observation that EcR is not expressed in Mamo$^{+}$ cells at the time α'β' neurons are produced (*i.e.*, from mid L3) suggests that ecdysone signaling does not function in α'β' specification and does not regulate Mamo. The lack of a role for ecdysone in α'β' specification is consistent with our observations that expression of *UAS-EcR-RNAi* or mutants for *usp* do not disrupt α'β' specification. In contrast, we and others have shown that expression of *UAS-EcR-DN* leads to the loss of α'β' neurons (Marchetti and Tavosanis, 2017) However, since we cannot detect EcR protein in Mamo$^{+}$ cells at L3 and only *UAS-EcR-DN* blocks α'β' specification by inhibiting Mamo at L3, we conclude that EcR-DN artifactually represses Mamo, leading to the loss of α'β' neurons.

**Glia are a source of the Activin ligand Myoglianin**

*myo* is temporally expressed in brain glia at L3 to initiate the remodeling of mushroom body γ neurons (Awasaki et al., 2011) and α'β' specification (Fig. 4) (Marchetti and Tavosanis, 2019). However, knocking-down Myo from glia is not as severe as removing Babo from mushroom body neuroblasts. This might be due to incomplete knockdown of *myo* or to other sources of Myo, potentially from neurons. In the vertebrate cortex, old neurons signal back to young neurons to control their number (Parthasarathy et

al., 2014; Seuntjens et al., 2009; Toma et al., 2014; Wang et al., 2016). It is also possible the Babo is activated by other Activin ligands, including Activin and Dawdle (Upadhyay et al., 2017).

**Conserved mechanisms of temporal patterning**

It is well established that extrinsic cues play important roles during vertebrate neurogenesis, either by regulating temporal competence of neural stem cells or by controlling the timing of temporal identity transitions (reviewed in Kawaguchi, 2019). Competence changes mediated by extrinsic cues were demonstrated in classic heterochronic transplantation studies that showed that young donor progenitors produce old neuronal types when placed in older host brains. (Desai and McConnell, 2000; Frantz and McConnell, 1996; McConnell, 1988). Recent studies show that the reverse is also true when old progenitors are placed in a young environment (Oberst et al., 2019).

Mechanisms of intrinsic temporal patterning are also conserved (Alsio et al., 2013; Elliott et al., 2008; Holguera and Desplan, 2018; Konstantinides et al., 2015; Mattar et al., 2015; Shen et al., 2006). For example, vertebrate retinal progenitor cells use an intrinsic tTF cascade to bias young, mid, and old retinal fates (Elliott et al., 2008; Liu et al., 2020; Mattar et al., 2015). Two of the factors (Ikaros and Casz1) used for intrinsic temporal patterning are orthologs to the *Drosophila* tTFs Hb and Cas. tTF series might also exist in cortical radial glia progenitors and even in the nerve cord (Delile et al., 2019; Gao et al., 2014; Llorca et al., 2019; Telley et al., 2016, 2019). Recent results also show the importance of post-transcriptional regulation in defining either young or old cortical fates (Shu et al., 2019; Zahr et al., 2018), which can be compared to the use of posttranscriptional regulators that are a hallmark of neuronal temporal patterning in *Drosophila* central brain neuroblasts. These studies highlight that the mechanisms driving the diversification of neuronal types are conserved.

**Acknowledgements:**

We would like to thank the fly community, the Bloomington and the DGRC stock centers for flies and reagents; Nikos Konstantinides for discussion throughout the project and comments on the manuscript. Tzumin Lee for sharing data prior to publication and for discussions; Tzumin Lee, Lynn Riddiford, Oren Schuldine, Cedric Maurange and Michael B. O'Connor for fly stocks and antibodies. We would like to thank all the Desplan lab members for their discussion and comments on the manuscript; Funding: This work was supported by grants from NIH (R01 EY017916 and R21 NS095288). A.M.R. was partly supported by funding from NIH (T32 HD007520), and by NYU's GSAS MacCracken Program and a Dean's Dissertation Fellowship.

**Author contributions:**

Conceptualization, A.M.R. and C.D.; Investigation, A.M.R.; Writing - Original Draft, A.M.R.; Writing - Review and Editing, A.M.R. and C.D.; Data and materials availability: All data are available in the main text or supplementary materials.

**Declaration of Interests:**

The authors declare no competing interests.

**Figure titles and legends:**

**Fig. 1. α'β' neurons are not generated from *babo* mutant neuroblasts. A.** Summary of intrinsic temporal patterning mechanism operating during mushroom body development. During early larval stages, mushroom body neuroblasts express high levels of Imp (red) and Chinmo (red) in neurons to specify γ identity for ~85 neuroblast divisions (red-dashed box). From mid L3 to metamorphosis, when Imp and Syp (cyan) are both at low levels, the same neuroblast divides ~40 times to produce α'β' neurons (magenta-dashed box). Low Chinmo regulates the expression Mamo, a terminal selector of α'β' identity. From the beginning of metamorphosis throughout pupal development, high Syp leads to αβ neurons

(cyan-dashed outline). **B.** Known molecular markers can distinguish between the three mushroom body neuronal types in the adult. **C.** Mushroom body projections originating from neurons born from four neuroblasts (numbered 1 to 4) per hemisphere fasciculate into a single bundle (peduncle) before branching into the five mushroom body lobes. The first-born γ neurons (red) remodel during development to project into a single, medial lobe in the adult. This lobe is the most anterior of the medial lobes. Axons from α'β' neurons (magenta) bifurcate to project into the vertical and medial α' and β' lobes. The β' lobe is posterior to the γ lobe. The last-born αβ neurons (cyan) also bifurcate their axons into the vertical projecting α lobe and medial projecting β lobe. The α lobe is positioned adjacent and medial to the α' lobe. The β lobe is the most posterior medial lobe. **D-E.** Representative max projections showing adult axons of clonally related neurons born from L1 stage in wildtype and *babo* conditions. *UAS-CD8::GFP* is driven by *mb-Gal4* (*OK107-Gal4*). Outlines mark $GFP^+$ axons, where γ axons are outlined in red, α'β' axons are outlined in magenta, and αβ axons are outlined in cyan. A white box outlines the Inset panel. Trio (magenta) is used to label all γ and α'β' axons for comparison to $GFP^+$ axons. **D.** In wildtype, $GFP^+$ axons (green, outlined in red, magenta and cyan) are visible in all observable mushroom body lobes. **E.** In *babo* mutant clones, γ neurons (red outline) remain unpruned. $GFP^+$ axons are missing inside the $Trio^+$ α' lobe, indicating the absence of α'β' neurons. **F-G.** Representative, single z-slices from the adult cell body region of clones induced at L1 in wildtype and *babo* conditions. *UAS-CD8::GFP* is driven by *mb-Gal4*. **F.** Wildtype clones show the presence of strongly expressing Trio (magenta) and Mamo (blue, gray in single channel) neurons, indicative of α'β' identity. **G.** In *babo* mutant clones, cells strongly expressing Trio and Mamo are not present. **H.** Quantification of MARCM clones marked by *mb-Gal4*, which labels all mushroom body neuronal types. The number of α'β' neurons are quantified in wildtype (n=7) and *babo* (n=8) conditions. Plotted is the percentage of strong $Mamo^+$ and $GFP^+$ cells (clonal cells) versus all $Mamo^+$ cells (clonal and non-clonal cells) within a single mushroom body. In wildtype, 25.5% of the total strong Mamo expressing cells (α'β' neurons) are within a clone, consistent with our expectation since each mushroom body is made from four neuroblasts. In *babo* clones, only 2.2% of α'β' neurons are

within a clone. **H'.** There are no significant differences between the average clone sizes (wildtype:533.6; *babo*:551.3). **I.** Quantification of γ neurons marked by *γ-Gal4* (*71G10-Gal4*) in MARCM clones. Plotted is the total number of γ neurons marked by GFP and Trio in wildtype (n=10) and *babo* mutant (n=12) clones. In wildtype, the average number of γ neurons is 154.3. In *babo* mutants, the average is 178.4. **J.** Quantification of α'β' neurons marked by *α'β'-Gal4* (*41C07-Gal4*) in MARCM clones. Plotted is the total number of α'β' neurons marked by GFP and strong Trio in wildtype (n=4) and *babo* mutant (n=8) clones. In wildtype, the average number of α'β' neurons is 81.5. In *babo* mutants, the average is 2.1. **K.** Quantification of αβ neurons marked by *αβ-Gal4* (*44E04-Gal4*) in MARCM clones. Plotted is the total number of $GFP^+$ cells in wildtype (n=7) and *babo* mutant (n=8) clones. In wildtype, the average number is 276. In *babo* mutants, the average number is 228.9. A two-sample, two-tailed t-test was performed. ***p<0.001, **p<0.01, ns: not significant. Scale bars: D, 20μm; F, 5μm.

**Fig. 2. Activin signaling acts in neuroblasts to lower Imp levels. A.** Representative image of a *babo* mushroom body neuroblast marked by *UAS-CD8::GFP* driven by *mb-Gal4* (red box) adjacent to a wildtype neuroblast (green-dashed box) in the same focal plane from a wandering L3 stage brain, immunostained for Imp (blue, gray in single channel) and Syp (magenta). **B.** Close-up view of wildtype neuroblast (green-dashed box in **A**). **C.** Close up view of *babo* mutant neuroblast (red box in **A**). **D.** Quantification of the Imp to Syp ratio in *babo* neuroblasts (n=9 from 4 different brains) compared to wildtype (n=23 from the same 4 brains as *babo* neuroblasts). A two-sample, two-tailed t-test was performed. ***p<0.001, ns: not significant. Scale bar: 10μm.

**Fig. 3. Activin signaling is sufficient to expand production of α'β' neurons. A.** Expression of *UAS-Babo-Act* by *mb-Gal4* leads to additional α'β' neurons but does not convert all mushroom body neurons into this fate. **B.** Plotted is the percentage of strong $Mamo^+$ and $GFP^+$ cells (clonal cells) versus all $Mamo^+$ cells (clonal and non-clonal cells) within a single mushroom body. The number of α'β' neurons is

quantified in wildtype (n=7, replotted from data in Figure 1H ) and *UAS-babo-Act* (n=4). In wildtype, 25.5% of the total strong Mamo expressing cells (α'β' neurons) are within a clone while precociously activating the Activin pathway increased the percentage to 32%. **C.** A representative image of a wandering L3 brain in which a single mushroom body neuroblast is expressing *UAS-babo-Act* driven by *mb-Gal4* (white-dashed line). Imp (blue) and Syp (magenta), along with GFP (green), are used to identify mushroom body neuroblasts (asterisks). **D.** Inset (gray box in **C**) showing that Mamo (gray) is expressed inside $GFP^+$ cells that express *UAS-babo-Act* but not outside in adjacent wildtype mushroom body neurons (yellow line) (n=3/3). A two-sample, two-tailed t-test was performed. ***p<0.001.

**Fig. 4. Glia are the source of the Activin ligand Myo to specify α'β' neurons. A-B.** Representative images of adult mushroom body lobes labeled by FasII (green) and Trio (magenta). **A.** In wildtype controls (428.9, (n=10) (*repo-Gal4* only) all three neuronal types are present based on axonal projections. **B.** Expressing *UAS-myo-RNAi* (106.6, n=10) causes γ neurons not to remodel and to the loss of the majority of α'β' neurons, however some still remain (purple arrow, FasII- region). **C-D.** Representative images of adult mushroom body cell body region. Trio (magenta) and Mamo (gray) are used to distinguish between the three neuronal types. Expressing *UAS-myo-RNAi* leads to loss of the majority of strong Mamo+ and $Trio^+$ cells, indicating the loss of α'β' neurons. **E.** Quantification of phenotype presented in **A-D**. **F.** At L3, EcR (magenta) and Mamo (gray) are expressed in mushroom body neurons labeled by Eyeless (green, yellow outline). $Mamo^+$ cells are α'β' neurons. **G.** Expressing *UAS-myo-RNAi* with *repo-Gal4* leads to loss of both Mamo and EcR in mushroom body neurons. A two-sample, two-tailed t-test was performed. ***p<0.001.

**Fig. 5. α'β' neurons are specified by low Imp levels at L3. A-A'.** Representative image of wildtype mushroom body neurons labeled by *mb-Gal4* driving *UAS-CD8::GFP* (green, white-dashed outline) during the wandering L3 stage. Mamo (gray) is used as a marker for α'β' neurons. **B-B'.** When *mb-Gal4*

is used to drive *UAS-Imp-RNAi*, Mamo is not expressed. **C-C'.** Similarly, Mamo expression is lost when overexpressing *Imp* (*UAS-Imp-overexpression* (*OE*)). **D-D'.** Expressing *UAS-Syp-RNAi* also leads to the loss of Mamo. **E.** Expressing *UAS-Syp-overexpression* (*OE*) does not affect Mamo. Scale bar: 5µm.

**Fig. 6. Ecdysone signaling is not necessary for α'β' specification. A-B.** Representative max projections showing adult axons of clonally related neurons born from L1 stage in wildtype and *UAS-EcR-DN* conditions. *UAS-CD8::GFP* is driven by *mb-Gal4* (*OK107-Gal4*). Outlines mark $GFP^+$ axons, where γ axons are outlined in red, α'β' axons are outlined in magenta, and αβ axons are outlined in cyan. A white box outlines the Inset panel. Trio (magenta) is used to label all γ and α'β' axons for comparison to $GFP^+$ axons. **A.** In wildtype, $GFP^+$ axons are visible in all mushroom body lobes. **B.** α'β' axons are lost, and γ neurons do not remodel, in *UAS-EcR-DN* expressing clones. **C-D.** Representative, single z-slices from the adult cell body region of clones induced at L1 in wildtype and *UAS-EcR-DN* conditions. *UAS-CD8::GFP* is driven by *mb-Gal4*. **C.** Wildtype clones show the presence of strongly expressing Trio (magenta) and Mamo (blue, gray in single channel) neurons, indicative of α'β' identity. **D.** In *UAS-EcR-DN* clones, strong Trio and Mamo cells are not present. **E.** Quantification of MARCM clones marked by *mb-Gal4*, which labels all mushroom body neuronal types. The number of α'β' neurons are quantified in wildtype (n=7, replotted from data in Figure 1H) and *UAS-EcR-DN* (n=6) conditions. Plotted is the percentage of strong $Mamo^+$ and $GFP^+$ cells (clonal cells) versus all $Mamo^+$ cells (clonal and non-clonal cells) within a single mushroom body. In wildtype, 25.5% of the total strong Mamo expressing cells (α'β' neurons) are within a clone. In *UAS-EcR-DN* clones, only 3.4% of α'β' neurons are within a clone. **F.** *usp* mutant clones contain α'β' neurons. FasII (magenta) is used to label γ and αβ lobes. Red arrow indicates unpruned γ neurons. **G.** Representative image of an *UAS-EcR-DN* expressing neuroblast marked by *UAS-CD8::GFP* driven by *mb-Gal4* (red box) ventral to a wildtype neuroblast (green-dashed box) from the same wandering L3 stage brain, immunostained for Imp (blue, gray in single channel) and Syp (magenta). **H.** Close-up view of wildtype neuroblast (green-dashed box in **G**). **I.** Close-up view of *UAS-EcR-DN*

neuroblast (red box in **G**). **J.** Quantification of the Imp to Syp ratio in *UAS-EcR-DN* neuroblasts (n=4 from 4 different brains) compared to wildtype (n=27 from the same 4 brains as *UAS-EcR-DN* neuroblasts). **K.** A representative adult mushroom body clone (green) induced at L1 expressing *UAS-EcR-DN* driven by *mb-Gal4*. α'β' neurons ($GFP^+$ (green), FasII- (magenta)) are not observed and γ neurons do not remodel ($GFP^+$, $FasII^+$, red outline). **L.** A representative adult wildtype clone induced at L1 driven by *NB + mb2-Gal4*. All three neuron types are present, including α'β' neurons ($GFP^+$, $FasII^-$, magenta outline). **M.** α'β' neurons are also present when *UAS-EcR-DN* is driven by *NB + mb2-Gal4* although γ neurons do not remodel. **N.** Quantification of MARCM clones in which *UAS-EcR-DN* is driven by *mb-Gal4* (n=6, replotted from data in **E**) or *NB + mb2-Gal4* (n=6) compared to wildtype (n=7, replotted from data in Figure 1H). In *UAS-EcR-DN* clones driven by *NB + mb2-Gal4*, 24.6% of α'β' neurons are within a clone, similar to wildtype. **O.** At L3, Mamo (gray) is expressed in young mushroom body neurons (α'β') while EcR (magenta) can only be detected in more mature neurons (mainly γ at this stage). **P.** Expressing *UAS-EcR-DN* with *mb-Gal4* (green, white outline) leads to the loss of Mamo expression (gray) inside the clone but not in surrounding wildtype mushroom body neurons. **Q.** In contrast, expressing *UAS-EcR-RNAi* driven by *mb-Gal4* abolishes EcR expression but does not affect Mamo. For **E** and **J** a two-sample, two-tailed t-test was performed. For **N**, a Tukey test was performed. ***p<0.001, ns: not significant. Scale bars: A, 20μm; G, 10μm; P, 5μm.

**Fig. 7. Model of how Activin signaling defines the α'β' temporal identity window.** In wildtype, as development proceeds, mushroom body neuroblasts incorporate an Activin signal (Myo) from glia through Babo to lower the level of the intrinsic temporal factor Imp (magenta dashed line). The lower Imp levels inherited by newborn neurons leads to lower Chinmo levels to control the expression of the α'β' effector Mamo, defining the mid-temporal window (magenta dashed lines). In *babo* mutants, Imp remains higher for longer, leading to the loss of Mamo (and likely many other targets) during mid-late L3 in

neurons. In this scenario, γ neuron numbers increase, α'β' neurons are lost, and fewer αβ neurons are produced. The Imp to Syp transition still occurs, allowing for young (γ) and old (αβ) fates to be produced.

## Methods:

### *Drosophila* strains and MARCM

Flies were kept on standard cornmeal medium at 25°C. For MARCM experiments, embryos were collected every 12 hours. After 24 hours, L1 larvae were placed at 37°C for 2 hours for neuroblast clones or 15 minutes for GMC clones. To target GMCs at L3, larvae were aged for 84 hours and then placed at 37°C for 15 minutes. Brains were dissected from 1-5 day old adults.

We used the following transgenic and mutant flies in combination or recombined in this study. {} enclose individual genotypes, separated by commas. Stock numbers refers to BDSC unless otherwise stated: {*y, w, UAS-mCD8::GFP, hsFlp; FRTG13, tub-Gal80/CYO; ; OK107-Gal4* (gift from Oren Schuldiner)}, {*hsFLP, y, w; FRTG13, UAS-mCD8::GFP* (#5131)}, {*hsFLP, tubP-GAL80, w, FRT19A; UAS-mCD8::GFP/CyO; OK107-Gal4* (#44407)}, {*hsFLP, y, w, UAS-mCD8::GFP; FRT82B, tubP-GAL80/TM3, $Sb^1$; OK107-Gal4* (#44408)}, {*hsFLP, $y^1$, w*, UAS-mCD8::GFP; tubP-GAL80, FRT40A; OK107-Gal4* (#44406)}, {*UAS-EcR.B1-DeltaC655.W650A* (#6872)}, {*y, w, FRT19A* (#1744)}, {*FRTG13, $babo^{52}$* (gift from Dr. Michael B. O'Connor)}, {*w; FRTG13* (#1956)}, {*w1118; repo-Gal4/TM3, $Sb^1$* (#7415)}, {w; *GMR71G10-GAL4* (#39604)}, {w; *GMR41C07-GAL4/TM3, $Sb^1$* (#48145)}, {*w; GMR13F02-GAL4* (#48571)}, {*w; GMR44E04-GAL4* (#50210)}, {*w*; insc-Gal4$^{Mz1407}$* (#8751)}, {*$usp^2$/FM7a* (#31414)}, {*$Met^{27}$, $gce^{2.5K}$/FM7c, 2x$Tb^1$-RFP, $sn^+$* (gift from Dr. Lynn Riddiford)}, {*$y^{d2}$, $w^{1118}$, ey-FLP; $tai^{EY11718}$ FRT40A/CyO, $y^+$* (DGRC #114680)}, {*$dpy^{ov1}$, $tai^{61G1}$, FRT40A/CyO* (#6379)}, {*w*; $smo^{119B6}$, $al^1$, $dpy^{ov1}$, $b^1$, FRT40A/CyO* (#24772)}, {*FRT82B, $svp^1$/TM3* (gift from Tzumin Lee)}, {*$y^1$, w*, UAS-mCD8::GFP, $Smox^{MB388}$, FRT19A/FM7c* (#44384)}, {*w*;; UAS-p35* (#5073)}, {*$y^1$, w; Mi{PT-GFSTF.1}EcR[MI05320-GFSTF.1]/SM6a,* (#59823)}, {*$y^1$, w*; $Pin^{Yt}$/CyO; UAS-mCD8::GFP* (#5130)},

{*w*; ; UAS-EcR.B1* (#6469)}, {*y, w; ; UAS-babo-a/TM6* (gift from Dr. Michael O'Connor)}, {*UAS-Imp-RNAi* (#34977)}, {*UAS-Imp-RM-Flag* (gift from Dr. Tzumin Lee)}, {*UAS-Syp-RNAi* (VDRC 33012, gift from Dr. Tzumin Lee)}, {*UAS-Syp-RB-HA* (gift from Dr. Tzumin Lee)}, {$y^1$, $v^1$*; UAS-myoglianin-RNAi* (#31200)}, {*w*; OK107-Gal4 /*$In^4$, $ci^D$ (#854)}; {*w, UAS-EcR-RNAi* (#9326)}; {*w, UAS-EcR-RNAi* (#9327)}; {*yw, UAS-babo.Q302D* (#64293)}.

**Immunohistochemistry and microscopy**

Fly brains were dissected in ice-cold PBS and fixed for 15-20 minutes in 4% Formaldehyde (v/w) in 1XPBS. Following a 2 hour wash in PBST (1XPBS + 0.3% Triton X-100), brains were incubated for 1-2 days in primary antibodies diluted in PBST, followed by overnight with secondary antibodies diluted in PBST. After washes, brains were mounted in Slowfade (Life Technologies) and imaged on either a Leica SP5 or SP8 confocal. Images were processed in Fiji and Adobe Illustrator (CC18).

We used the following antibodies in this study:

sheep anti-GFP (1:500, Bio-Rad #4745-1051), mouse anti-Trio (1:50, DSHB #9.4A anti-Trio), guinea pig anti-Mamo (1:200, this study, Genscript), mouse anti-FasII (1:50, DSHB #1D4 anti-Fasciclin II), rat anti-Imp (1:200, this study, Genscript), rabbit anti-Syp (1:200, this study, Genscript), guinea pig anti-Dpn (1:1000, Genscript), rabbit anti-FasII (1:50, this study, Genscript), mouse anti-EcR-B1 (1:20, DSHB #AD4.4(EcR-B1)), mouse anti-Dac2-3 (1:20, DSHB #mAbdac2-3), guinea pig anti-Chinmo (1:200, this study, Genscript), rat anti-Chinmo (1:200, gift from Dr. Cedric Maurange ), rat anti-DNcad (1:20, DSHB #DN-Ex #8), donkey anti-sheep Alexa 488 (1:500, Jackson ImmunoResearch #713-545-147), donkey anti-mouse Alexa 555 (1:400, Thermo Scientific #A-31570), donkey anti-rabbit Alexa 555 (1:400, Thermo Scientific #A-31572), donkey anti-rat Alexa 647 (1:400, Jackson Immunochemicals #712-605-153), donkey anti-guinea pig Alexa 647 (1:400, Jackson Immunochemicals #706-605-148), donkey anti-rabbit 405 (1:100, Jackson Immunochemicals #711-475-152), donkey anti-rat Cy3 (1:400, Jackson

Immunochemicals #712-165-153), donkey anti-mouse 405 (1:100, Jackson Immunochemicals # #711-475-150).

Polyclonal antibodies were generated by Genscript (https://www.genscript. com/). The epitopes used for each immunization are listed below.

Mamo: amino acids 467-636 of the full length protein:

MDDRLEQDVDEEDLDDDVVVVGPATAMARGIAQRLAHQNLQRLHHTHHHAQHQHSQHHHPH
SQHHHTPHHQQHHTHSDDEDAMPVIAKSEILDDDYDDEMDLEDDDEADNSSNDLGLNMKMGS
GGAGGGGGVDLSTGSTLIPSPLITLPSSSAAAAAAAAAAMESQRSTPHHHHHH

Imp: amino acids 76-455 (of isoform PB) of the full length protein:

ADFPLRILVQSEMVGAIIGRQGSTIRTITQQSRARVDVHRKENVGSLEKSITIYGNPENCTNACKRI
LEVMQQEAISTNKGEICLKILAHNNLIGRIIGKSGNTIKRIMQDTDTKITVSSINDINSFNLERIITVK
GLIENMSRAENQISTKLRQSYENDLQAMAPQSLMFPGLHPMAMMSTPGNGMVFNTSMPFPSCQ
SFAMSKTPASVVPPVFPNDLQETTYLYIPNNAVGAIIGTRGSHIRSIMRFSNASLKIAPLDADKPLD
QQTERKVTIVGTPEGQWKAQYMIFEKMREEGFMCGTDDVRLTVELLVASSQVGRIIGKGGQNV
RELQRVTGSVIKLPEHALAPPSGGDEETPVHIIGLFYSVQSAQRRIRAMML

Syp: amino acids 35-231(of isoform PA) of the full length protein:

MAEGNGELLDDINQKADDRGDGERTEDYPKLLEYGLDKKVAGKLDEIYKTGKLAHAELDERAL
DALKEFPVDGALNVLGQFLESNLEHVSNKSAYLCGVMKTYRQKSRASQQGVAAPATVKGPDED
KIKKILERTGYTLDVTTGQRKYGGPPPHWEGNVPGNGCEVFCGKIPKDMYEDELIPLFENCGIIW
DLRLMM

FasII: amino acids 770-873 (of isoform PA) of the full length protein:

MHHHHHHDLLCCITVHMGVMATMCRKAKRSPSEIDDEAKLGSGQLVKEPPPSPLPLPPPVKLGG SPMSTPLDEKEPLRTPTGSIKQNSTIEFDGRFVHSRSGEIIGKNSAV

Chinmo: amino acids 494-604 (of isoform PF) of the full length protein:

MLNVWNATKMNNKNSVNTADGKKLKCLYCDRLYGYETNLRAHIRQRHQGIRVPCPFCERTFTR NNTVRRHIAREHKQEIGLAAGATIAPAHLAAAAAASAAATAAAS NHSPHHHHHH

**Cell counts quantification**

All confocal images were taken with a step size of three microns. Using Fiji, each image was cropped to limit the area to a region containing mostly mushroom body cell bodies. In all cases, $GFP^+$ cells were manually counted. To count α'β' neurons, images were split into their individual channels and the channel containing Mamo staining was automatically binarized to account for weak and strong Mamo expression using either Default or RenyiEntropy thresholding. Binarized images were processed further using the Watershed method to differentiate between contacting cells. The number of particles (*i.e.*, strong Mamo cells) measuring between 50-infinity squared pixels were automatically counted using the Analyze Particles function and a separate channel containing bare outlines of the counts was produced and inverted. This method automatically produced the total number of strong $Mamo^+$ cells. Individual channels were then remerged. Outlines drawn from the Analyze Particles function that overlapped with $GFP^+$ cells were defined as α'β' neurons within a clone. In the eight cases where two mushroom body neuroblasts were labeled in a single hemisphere (wildtype:1; *babo*, *UAS-EcR*: 3; *babo*, *UAS-Syp*: 2), the total number of α'β' neurons within clones was divided by 2.

**Imp and Syp fluorescence quantification**

All brains used for quantifying Imp and Syp fluorescence values in *babo* or *UAS-EcR-DN* mutants were prepared together. Additionally, all images used for quantification were imaged using the same confocal

settings for each channel. Fluorescence measurements were made in Fiji. Values for Imp and Syp were measured within the same hand-drawn area encompassing the entire neuroblast from a single z-slice.

**Statistics**

Statistical tests were performed in Excel or R. The exact tests used are reported in the figure legends. In all cases, whisker plots represent the minimum value (bottom whisker), first quartile (bottom of box to middle line), inclusive median (middle line), third quartile (middle line to top of box) and maximum value (top whisker). The "x" represents the average value. Outliers are 1.5 times the distance from the first and third quartile.

**References:**

Alsio, J.M., Tarchini, B., Cayouette, M., and Livesey, F.J. (2013). Ikaros promotes early-born neuronal fates in the cerebral cortex. Proc. Natl. Acad. Sci. *110*, E716–E725.

Alyagor, I., Berkun, V., Keren-Shaul, H., Marmor-Kollet, N., David, E., Mayseless, O., Issman-Zecharya, N., Amit, I., and Schuldiner, O. (2018). Combining Developmental and Perturbation-Seq Uncovers Transcriptional Modules Orchestrating Neuronal Remodeling. Dev. Cell *47*, 38-52.e6.

Aso, Y., Hattori, D., Yu, Y., Johnston, R.M., Iyer, N.A., Ngo, T.-T.B., Dionne, H., Abbott, L.F., Axel, R., Tanimoto, H., et al. (2014). The neuronal architecture of the mushroom body provides a logic for associative learning. Elife *3*, e04577.

Awasaki, T., Saito, M., Sone, M., Suzuki, E., Sakai, R., Ito, K., and Hama, C. (2000). The Drosophila trio plays an essential role in patterning of axons by regulating their directional extension. Neuron *26*, 119–131.

Awasaki, T., Huang, Y., O'Connor, M.B., and Lee, T. (2011). Glia instruct developmental neuronal remodeling through TGF-β signaling. Nat. Neurosci. *14*, 821–823.

Baumann, A.A., Texada, M.J., Chen, H.M., Etheredge, J.N., Miller, D.L., Picard, S., Warner, R., Truman, J.W., and Riddiford, L.M. (2017). Genetic tools to study juvenile hormone action in Drosophila. Sci. Rep.

*7*, 2132.

Briscoe, J., and Small, S. (2015). Morphogen rules: Design principles of gradient-mediated embryo patterning. Dev. *142*, 3996–4009.

Brummel, T., Abdollah, S., Haerry, T.E., Shimell, M.J., Merriam, J., Raftery, L., Wrana, J.L., and O'Connor, M.B. (1999). The Drosophila activin receptor Baboon signals through dSmad2 and controls cell proliferation but not patterning during larval development. Genes Dev. *13*, 98–111.

Cepko, C. (2014). Intrinsically different retinal progenitor cells produce specific types of progeny. Nat. Rev. Neurosci. *15*, 615–627.

Chai, P.C., Liu, Z., Chia, W., and Cai, Y. (2013). Hedgehog Signaling Acts with the Temporal Cascade to Promote Neuroblast Cell Cycle Exit. PLoS Biol. *11*.

Chleilat, E., Skatulla, L., Rahhal, B., Hussein, M.T., Feuerstein, M., Krieglstein, K., and Roussa, E. (2018). TGF-β Signaling Regulates Development of Midbrain Dopaminergic and Hindbrain Serotonergic Neuron Subgroups. Neuroscience *381*, 124–137.

Cognigni, P., Felsenberg, J., and Waddell, S. (2018). Do the right thing: neural network mechanisms of memory formation, expression and update in Drosophila. Curr. Opin. Neurobiol. *49*, 51–58.

Connolly, J.B., Roberts, I.J.H., Armstrong, J.D., Kaiser, K., Forte, M., Tully, T., and O'Kane, C.J. (1996). Associative learning disrupted by impaired Gs signaling in Drosophila mushroom bodies. Science (80-. ). *274*, 2104–2107.

Crittenden, J.R., Skoulakis, E.M.C., Han, K.-A., Kalderon, D., and Davis, R.L. (1998). Tripartite Mushroom Body Architecture Revealed by Antigenic Markers. Learn. Mem. *5*, 38–51.

Croset, V., Treiber, C.D., and Waddell, S. (2018). Cellular diversity in the Drosophila midbrain revealed by single-cell transcriptomics. Elife *7*, e34550.

Delile, J., Rayon, T., Melchionda, M., Edwards, A., Briscoe, J., and Sagner, A. (2019). Single cell transcriptomics reveals spatial and temporal dynamics of gene expression in the developing mouse spinal cord. Development *146*.

Desai, A.R., and McConnell, S.K. (2000). Progressive restriction in fate potential by neural progenitors

during cerebral cortical development. Development *127*, 2863–2872.

Dias, J.M., Alekseenko, Z., Applequist, J.M., and Ericson, J. (2014). Tgfβ Signaling Regulates Temporal Neurogenesis and Potency of Neural Stem Cells in the CNS. Neuron *84*, 927–939.

Doe, C.Q. (2017). Temporal Patterning in the Drosophila CNS. Annu. Rev. Cell Dev. Biol. *33*, 219–240.

Elliott, J., Jolicoeur, C., Ramamurthy, V., and Cayouette, M. (2008). Ikaros Confers Early Temporal Competence to Mouse Retinal Progenitor Cells. Neuron *60*, 26–39.

Frantz, G.D., and McConnell, S.K. (1996). Restriction of late cerebral cortical progenitors to an upper-layer fate. Neuron *17*, 55–61.

Gao, P., Postiglione, M.P., Krieger, T.G., Hernandez, L., Wang, C., Han, Z., Streicher, C., Papusheva, E., Insolera, R., Chugh, K., et al. (2014). Deterministic Progenitor Behavior and Unitary Production of Neurons in the Neocortex. Cell *159*, 775–788.

Hige, T. (2018). What can tiny mushrooms in fruit flies tell us about learning and memory? Neurosci. Res. *129*, 8–16.

Holguera, I., and Desplan, C. (2018). Neuronal specification in space and time. Science (80-. ). *362*, 176–180.

Homem, C.C.F., Steinmann, V., Burkard, T.R., Jais, A., Esterbauer, H., and Knoblich, J.A. (2014). Ecdysone and Mediator Change Energy Metabolism to Terminate Proliferation in Drosophila Neural Stem Cells. Cell *158*, 874–888.

Issman-Zecharya, N., and Schuldiner, O. (2014). The PI3K class III complex promotes axon pruning by downregulating a ptc-derived signal via endosome-lysosomal degradation. Dev. Cell *31*, 461–473.

Ito, K., Awano, W., Suzuki, K., Hiromi, Y., and Yamamoto, D. (1997). The Drosophila mushroom body is a quadruple structure of clonal units each of which contains a virtually identical set of neurones and glial cells. Development *124*, 761–771.

Jefferis, G.S.X.E., Marin, E.C., Stocker, R.F., and Luo, L. (2001). Target neuron prespecification in the olfactory map of Drosophila. Nature *414*, 204–208.

Jefferis, G.S.X.E., Potter, C.J., Chan, A.M., Marin, E.C., Rohlfing, T., Maurer, C.R., and Luo, L. (2007).

Comprehensive Maps of Drosophila Higher Olfactory Centers: Spatially Segregated Fruit and Pheromone Representation. Cell *128*, 1187–1203.

Jenett, A., Rubin, G.M., Ngo, T.T., Shepherd, D., Murphy, C., Dionne, H., Pfeiffer, B.D., Cavallaro, A., Hall, D., Jeter, J., et al. (2012). A GAL4-driver line resource for Drosophila neurobiology. Cell Rep *2*, 991–1001.

Kao, C.-F., Yu, H.-H., He, Y., Kao, J.-C., and Lee, T. (2012). Hierarchical Deployment of Factors Regulating Temporal Fate in a Diverse Neuronal Lineage of the Drosophila Central Brain. Neuron *73*, 677–684.

Kawaguchi, A. (2019). Temporal patterning of neocortical progenitor cells: How do they know the right time? Neurosci. Res. *138*, 3–11.

Kohwi, M., and Doe, C.Q. (2013). Temporal fate specification and neural progenitor competence during development. Nat. Rev. Neurosci. *14*, 823–838.

Konstantinides, N., Rossi, A.M., and Desplan, C. (2015). Common Temporal Identity Factors Regulate Neuronal Diversity in Fly Ventral Nerve Cord and Mouse Retina. Neuron *85*, 447–449.

Kraft, K.F., Massey, E.M., Kolb, D., Walldorf, U., and Urbach, R. (2016). Retinal homeobox promotes cell growth, proliferation and survival of mushroom body neuroblasts in the Drosophila brain. Mech. Dev. *142*, 50–61.

Kucherenko, M.M., Barth, J., Fiala, A., and Shcherbata, H.R. (2012). Steroid-induced microRNA let-7 acts as a spatio-temporal code for neuronal cell fate in the developing Drosophila brain. EMBO J. *31*, 4511–4523.

Kunz, T., Kraft, K.F., Technau, G.M., and Urbach, R. (2012). Origin of Drosophila mushroom body neuroblasts and generation of divergent embryonic lineages. Development *139*, 2510–2522.

Kurusu, M., Maruyama, Y., Adachi, Y., Okabe, M., Suzuki, E., and Furukubo-Tokunaga, K. (2009). A conserved nuclear receptor, Tailless, is required for efficient proliferation and prolonged maintenance of mushroom body progenitors in the Drosophila brain. Dev. Biol. *326*, 224–236.

Lee, T., and Luo, L. (1999). Mosaic analysis with a repressible neurotechnique cell marker for studies of

gene function in neuronal morphogenesis. Neuron *22*, 451–461.

Lee, T., Lee, A., and Luo, L. (1999). Development of the Drosophila mushroom bodies: sequential generation of three distinct types of neurons from a neuroblast. Development *126*, 4065–4076.

Lee, T., Marticke, S., Sung, C., Robinow, S., and Luo, L. (2000). Cell-autonomous requirement of the USP/EcR-B ecdysone receptor for mushroom body neuronal remodeling in Drosophila. Neuron *28*, 807–818.

Lee, Y.-J., Yang, C.-P., Miyares, R.L., Huang, Y.-F., He, Y., Ren, Q., Chen, H.-M., Kawase, T., Ito, M., Otsuna, H., et al. (2020). Conservation and divergence of related neuronal lineages in the Drosophila central brain. Elife *9*.

Lin, S., Lai, S.-L., Yu, H.-H., Chihara, T., Luo, L., and Lee, T. (2010). Lineage-specific effects of Notch/Numb signaling in post-embryonic development of the Drosophila brain. Development *137*, 43–51.

Liu, L., Long, X., Yang, C., Miyares, R.L., Sugino, K., Singer, R.H., and Lee, T. (2019). Mamo decodes hierarchical temporal gradients into terminal neuronal fate. Elife *8*, 1–28.

Liu, S., Liu, X., Li, S., Huang, X., Qian, H., Jin, K., and Xiang, M. (2020). Foxn4 is a temporal identity factor conferring mid/late-early retinal competence and involved in retinal synaptogenesis. Proc. Natl. Acad. Sci. 201918628.

Liu, Z., Yang, C.-P., Sugino, K., Fu, C.-C., Liu, L.-Y., Yao, X., Lee, L.P., and Lee, T. (2015). Opposing intrinsic temporal gradients guide neural stem cell production of varied neuronal fates. Science (80-. ). *350*, 317–320.

Llorca, A., Ciceri, G., Beattie, R., Wong, F.K., Diana, G., Serafeimidou-Pouliou, E., Fernández-Otero, M., Streicher, C., Arnold, S.J., Meyer, M., et al. (2019). A stochastic framework of neurogenesis underlies the assembly of neocortical cytoarchitecture. Elife *8*, 1–27.

Lodato, S., and Arlotta, P. (2015). Generating Neuronal Diversity in the Mammalian Cerebral Cortex. Annu. Rev. Cell Dev. Biol. *31*, 699–720.

Marchetti, G., and Tavosanis, G. (2017). Steroid Hormone Ecdysone Signaling Specifies Mushroom

Body Neuron Sequential Fate via Chinmo. Curr. Biol. *27*, 3017-3024.e4.

Marchetti, G., and Tavosanis, G. (2019). Modulators of hormonal response regulate temporal fate specification in the Drosophila brain. PLOS Genet. *15*, e1008491.

Mattar, P., Ericson, J., Blackshaw, S., and Cayouette, M. (2015). A Conserved Regulatory Logic Controls Temporal Identity in Mouse Neural Progenitors. Neuron *85*, 497–504.

McConnell, S.K. (1988). Fates of visual cortical neurons in the ferret after isochronic and heterochronic transplantation. J. Neurosci. *8*, 945–974.

McConnell, S.K., and Kaznowski, C.E. (1991). Cell cycle dependence of laminar determination in developing neocortex. Science *254*, 282–285.

Murthy, M., Fiete, I., and Laurent, G. (2008). Testing Odor Response Stereotypy in the Drosophila Mushroom Body. Neuron *59*, 1009–1023.

Oberst, P., Fièvre, S., Baumann, N., Concetti, C., Bartolini, G., and Jabaudon, D. (2019). Temporal plasticity of apical progenitors in the developing mouse neocortex. Nature *573*, 370–374.

Pahl, M.C., Doyle, S.E., and Siegrist, S.E. (2019). E93 Integrates Neuroblast Intrinsic State with Developmental Time to Terminate MB Neurogenesis via Autophagy. Curr. Biol. 1–13.

Parthasarathy, S., Srivatsa, S., Nityanandam, A., and Tarabykin, V. (2014). Ntf3 acts downstream of Sip1 in cortical postmitotic neurons to control progenitor cell fate through feedback signaling. Development *141*, 3324–3330.

Ren, Q., Yang, C.-P., Liu, Z., Sugino, K., Mok, K., He, Y., Ito, M., Nern, A., Otsuna, H., and Lee, T. (2017). Stem Cell-Intrinsic, Seven-up-Triggered Temporal Factor Gradients Diversify Intermediate Neural Progenitors. Curr. Biol. 1–11.

Rossi, A.M., Fernandes, V.M., and Desplan, C. (2017). Timing temporal transitions during brain development. Curr. Opin. Neurobiol. *42*, 84–92.

Seuntjens, E., Nityanandam, A., Miquelajauregui, A., Debruyn, J., Stryjewska, A., Goebbels, S., Nave, K.A., Huylebroeck, D., and Tarabykin, V. (2009). Sip1 regulates sequential fate decisions by feedback signaling from postmitotic neurons to progenitors. Nat. Neurosci. *12*, 1373–1380.

Shen, Q., Wang, Y., Dimos, J.T., Fasano, C.A., Phoenix, T.N., Lemischka, I.R., Ivanova, N.B., Stifani, S., Morrisey, E.E., and Temple, S. (2006). The timing of cortical neurogenesis is encoded within lineages of individual progenitor cells. Nat. Neurosci. *9*, 743–751.

Shih, M.-F.M., Davis, F.P., Henry, G.L., and Dubnau, J. (2019). Nuclear Transcriptomes of the Seven Neuronal Cell Types That Constitute the Drosophila Mushroom Bodies. G3 (Bethesda). *9*, 81–94.

Shu, P., Wu, C., Ruan, X., Liu, W., Hou, L., Fu, H., Wang, M., Liu, C., Zeng, Y., Chen, P., et al. (2019). Opposing Gradients of MicroRNA Expression Temporally Pattern Layer Formation in the Developing Neocortex. Dev. Cell *49*, 764-785.e4.

Siegrist, S.E., Haque, N.S., Chen, C.-H., Hay, B. a., and Hariharan, I.K. (2010). Inactivation of Both foxo and reaper Promotes Long-Term Adult Neurogenesis in Drosophila. Curr. Biol. *20*, 643–648.

Sipe, C.W., and Siegrist, S.E. (2017). Eyeless uncouples mushroom body neuroblast proliferation from dietary amino acids in *Drosophila*. Elife *6*, 1–10.

Sousa-Nunes, R., Cheng, L.Y., and Gould, A.P. (2010). Regulating neural proliferation in the Drosophila CNS. Curr. Opin. Neurobiol. *20*, 50–57.

Spana, E.P., and Doe, C.Q. (1996). Numb antagonizes Notch signaling to specify sibling neuron cell fates. Neuron *17*, 21–26.

Syed, M.H., Mark, B., and Doe, C.Q. (2017a). Steroid hormone induction of temporal gene expression in Drosophila brain neuroblasts generates neuronal and glial diversity. Elife *6*, 1–23.

Syed, M.H., Mark, B., and Doe, C.Q. (2017b). Playing Well with Others□: Extrinsic Cues Regulate Neural Progenitor Temporal Identity to Generate Neuronal Diversity. Trends Genet. *xx*, 1–10.

Telley, L., Govindan, S., Prados, J., Stevant, I., Nef, S., Dermitzakis, E., Dayer, A., and Jabaudon, D. (2016). Sequential transcriptional waves direct the differentiation of newborn neurons in the mouse neocortex. Science (80-. ). *351*, 1443–1446.

Telley, L., Agirman, G., Prados, J., Amberg, N., Fièvre, S., Oberst, P., Bartolini, G., Vitali, I., Cadilhac, C., Hippenmeyer, S., et al. (2019). Temporal patterning of apical progenitors and their daughter neurons in the developing neocortex. Science (80-. ). *364*, eaav2522.

Toma, K., Kumamoto, T., Hanashima, C., Toma, K., and Hanashima, C. (2014). The timing of upper-layer neurogenesis is conferred by sequential derepression and negative feedback from deep-layer neurons. J. Neurosci. *34*, 13259–13276.

Truman, J.W., Moats, W., Altman, J., Marin, E.C., and Williams, D.W. (2010). Role of Notch signaling in establishing the hemilineages of secondary neurons in Drosophila melanogaster. Development *137*, 53–61.

Turner, G.C., Bazhenov, M., and Laurent, G. (2008). Olfactory Representations by Drosophila Mushroom Body Neurons. J. Neurophysiol. *99*, 734–746.

Upadhyay, A., Moss-Taylor, L., Kim, M.-J., Ghosh, A.C., and O'Connor, M.B. (2017). TGF-β Family Signaling in Drosophila. Cold Spring Harb. Perspect. Biol. *9*, a022152.

Urbach, R., and Technau, G.M. (2004). Neuroblast formation and patterning during early brain development in Drosophila. Bioessays *26*, 739–751.

Vosshall, L.B., and Stocker, R.F. (2007). Molecular Architecture of Smell and Taste in Drosophila. Annu. Rev. Neurosci. *30*, 505–533.

Wang, W., Jossin, Y., Chai, G., Lien, W.H., Tissir, F., and Goffinet, A.M. (2016). Feedback regulation of apical progenitor fate by immature neurons through Wnt7-Celsr3-Fzd3 signalling. Nat. Commun. *7*, 1–11.

Wong, D.C., Lovick, J.K., Ngo, K.T., Borisuthirattana, W., Omoto, J.J., and Hartenstein, V. (2013). Postembryonic lineages of the Drosophila brain: II. Identification of lineage projection patterns based on MARCM clones. Dev. Biol. *384*, 258–289.

Wu, Y.-C., Chen, C.-H., Mercer, A., and Sokol, N.S. (2012). let-7-Complex MicroRNAs Regulate the Temporal Identity of Drosophila Mushroom Body Neurons via chinmo. Dev. Cell *23*, 202–209.

Yamanaka, N., Rewitz, K.F., and O'Connor, M.B. (2013). Ecdysone Control of Developmental Transitions: Lessons from Drosophila Research. Annu. Rev. Entomol. *58*, 497–516.

Yang, C.-P., Fu, C.-C., Sugino, K., Liu, Z., Ren, Q., Liu, L.-Y., Yao, X., Lee, L.P., and Lee, T. (2015). Transcriptomes of lineage-specific Drosophila neuroblasts profiled via genetic targeting and robotic sorting. Development.

Yang, C.-P.P., Samuels, T.J., Huang, Y., Yang, L., Ish-Horowicz, D., Davis, I., and Lee, T. (2017). Imp and Syp RNA-binding proteins govern decommissioning of Drosophila neural stem cells. Development *144*, 3454–3464.

Yu, H.-H., Kao, C.-F., He, Y., Ding, P., Kao, J.-C., and Lee, T. (2010). A Complete Developmental Sequence of a Drosophila Neuronal Lineage as Revealed by Twin-Spot MARCM. PLoS Biol. *8*, e1000461.

Yu, H.H., Awasaki, T., Schroeder, M.D., Long, F., Yang, J.S., He, Y., Ding, P., Kao, J.C., Wu, G.Y.Y., Peng, H., et al. (2013a). Clonal development and organization of the adult Drosophila central brain. Curr. Biol. *23*, 633–643.

Yu, X.M., Gutman, I., Mosca, T.J., Iram, T., Özkan, E., Garcia, K.C., Luo, L., and Schuldiner, O. (2013b). Plum, an immunoglobulin superfamily protein, regulates axon pruning by facilitating TGF-β signaling. Neuron *78*, 456–468.

Zahr, S.K., Yang, G., Kazan, H., Borrett, M.J., Yuzwa, S.A., Voronova, A., Kaplan, D.R., and Miller, F.D. (2018). A Translational Repression Complex in Developing Mammalian Neural Stem Cells that Regulates Neuronal Specification. Neuron *97*, 520-537.e6.

Zheng, X., Wang, J., Haerry, T.E., Wu, A.Y.-H., Martin, J., O'Connor, M.B., Lee, C.-H.J., and Lee, T. (2003). TGF-beta signaling activates steroid hormone receptor expression during neuronal remodeling in the Drosophila brain. Cell *112*, 303–315.

Zhu, S., Lin, S., Kao, C.-F., Awasaki, T., Chiang, A.-S., and Lee, T. (2006). Gradients of the Drosophila Chinmo BTB-Zinc Finger Protein Govern Neuronal Temporal Identity. Cell *127*, 409–422.

A

## Post-embryonic development (~9 days)

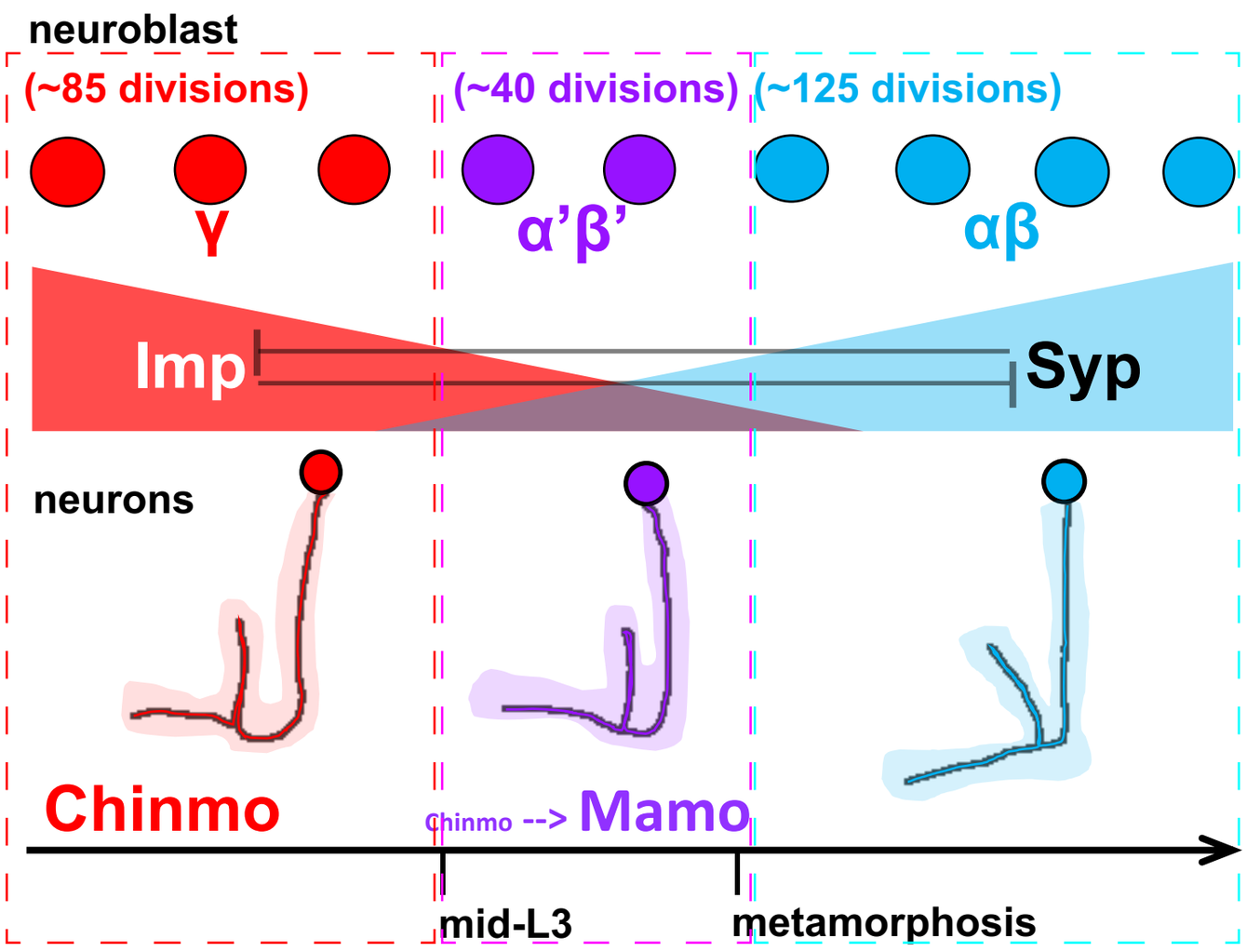


B

## Adult

| | γ | α'β' | αβ |
|---|---|---|---|
| Trio | + | ++ | |
| Mamo | + | ++ | |
| FasII (axons only) | + | | ++ |

C

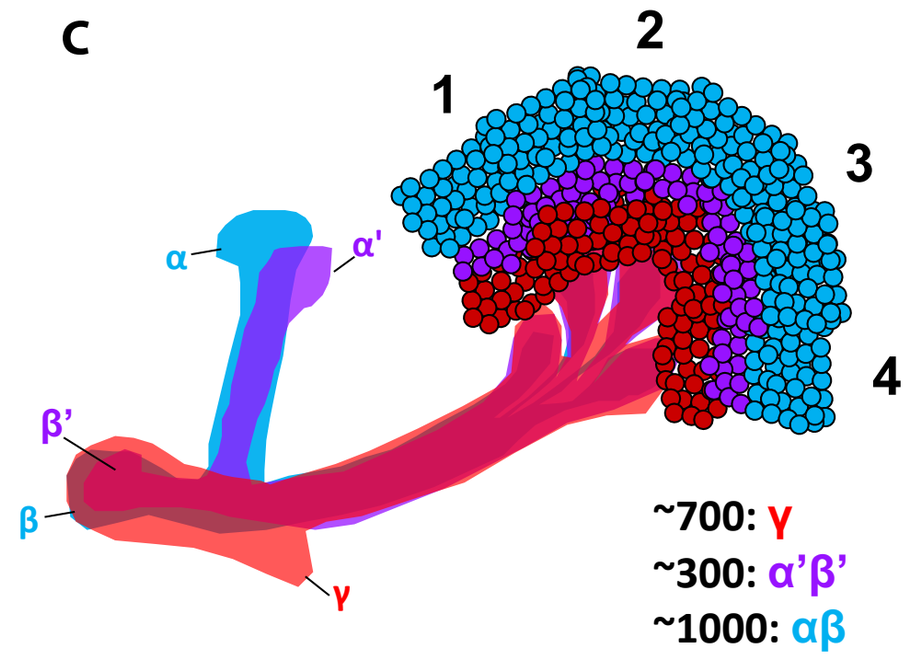


## Adult: *mb-Gal4* MARCM neuroblast clones induced at L1

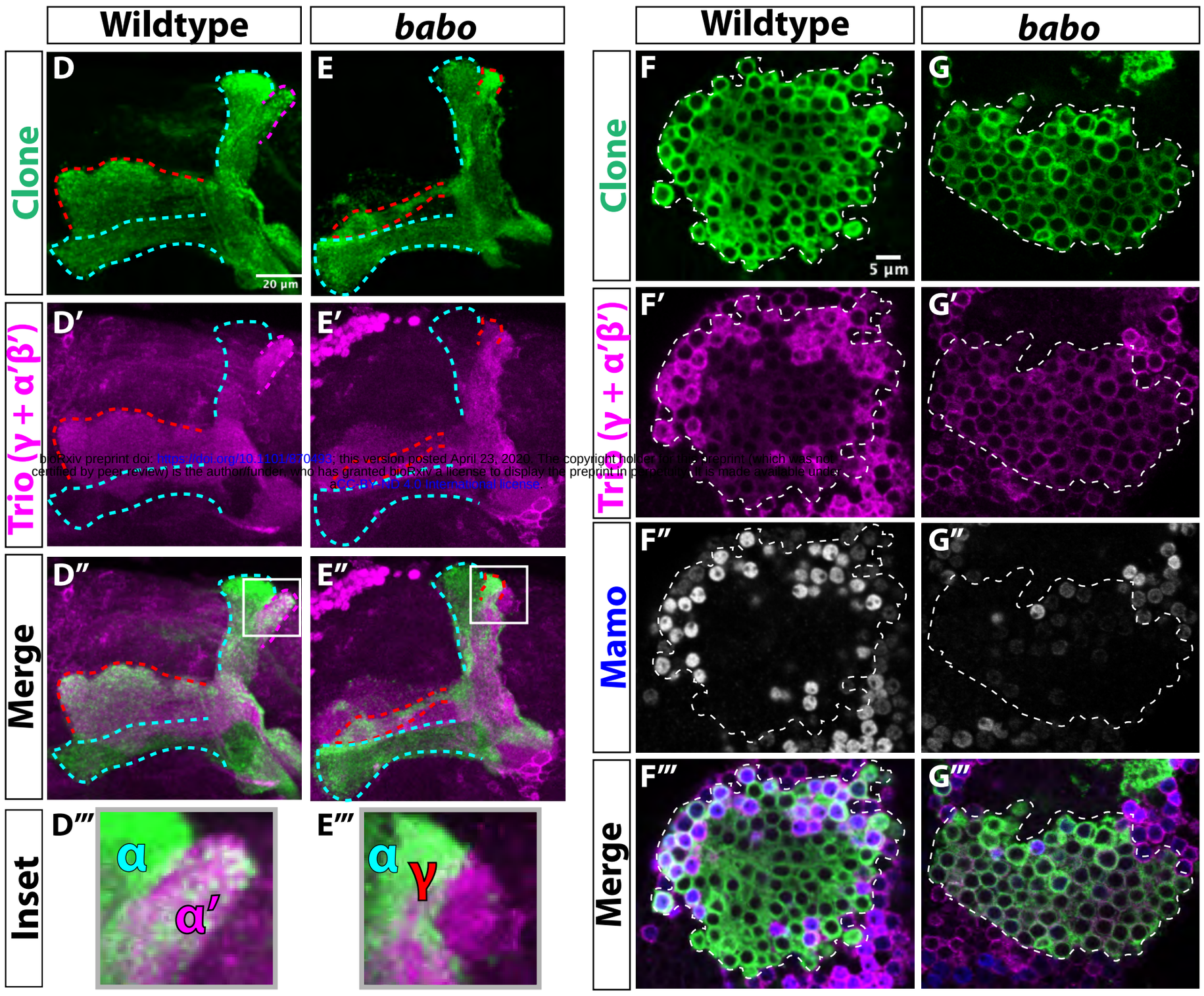




## *mb-Gal4 MARCM*

H

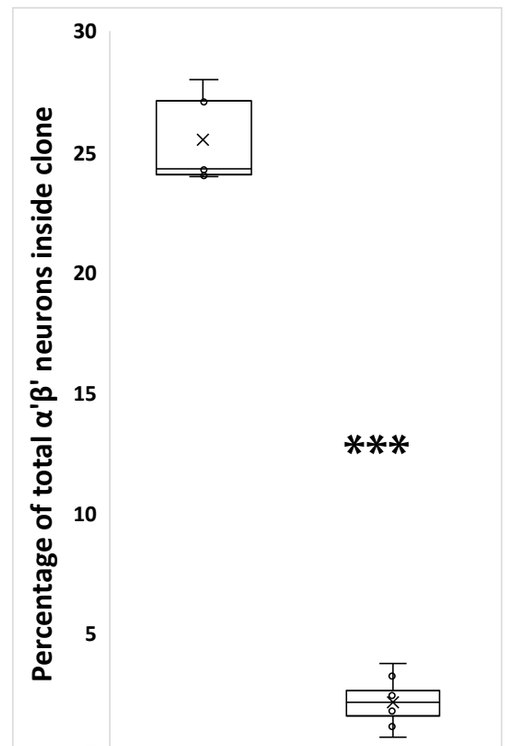


H'

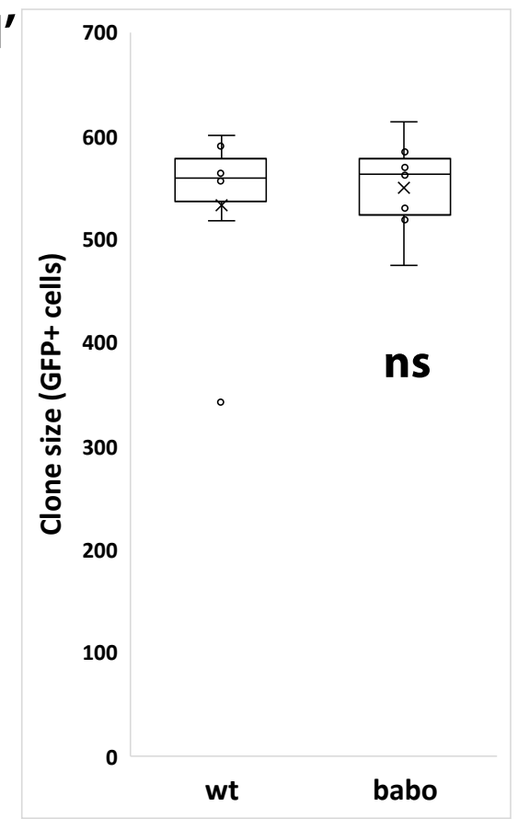


## Adult axonal morphology: γ, α'β', αβ

### *γ-Gal4 MARCM*

I

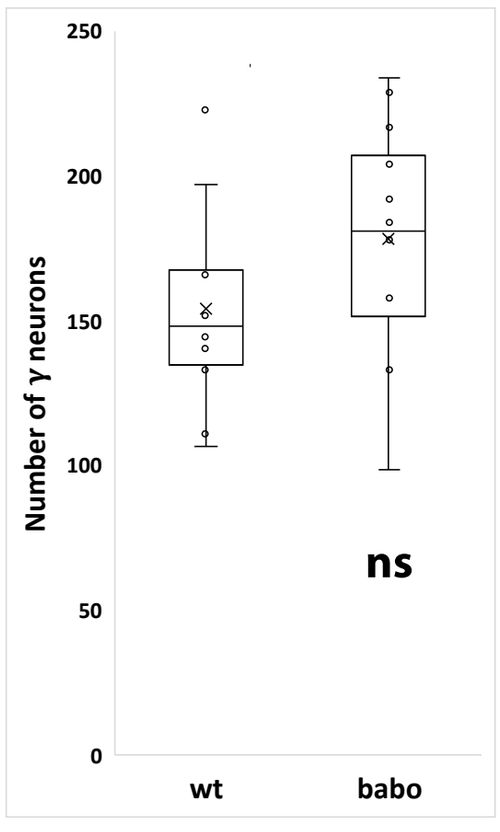


### *α'β'-Gal4 MARCM*

J

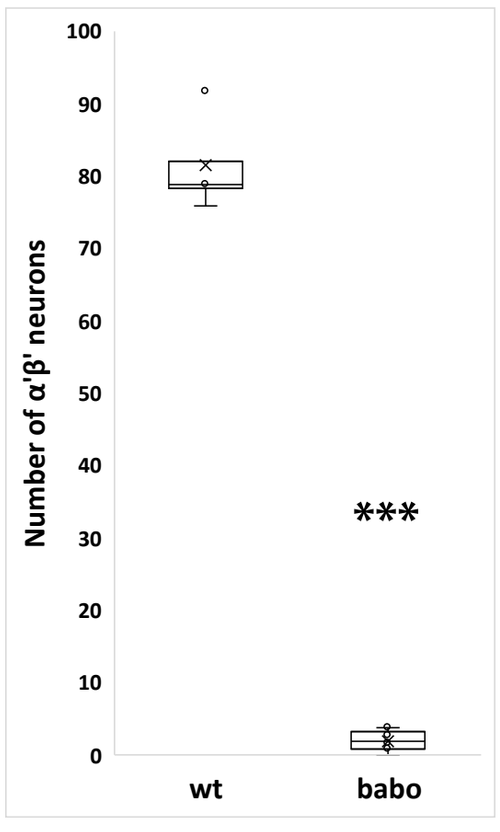


### *αβ-Gal4 MARCM*

K

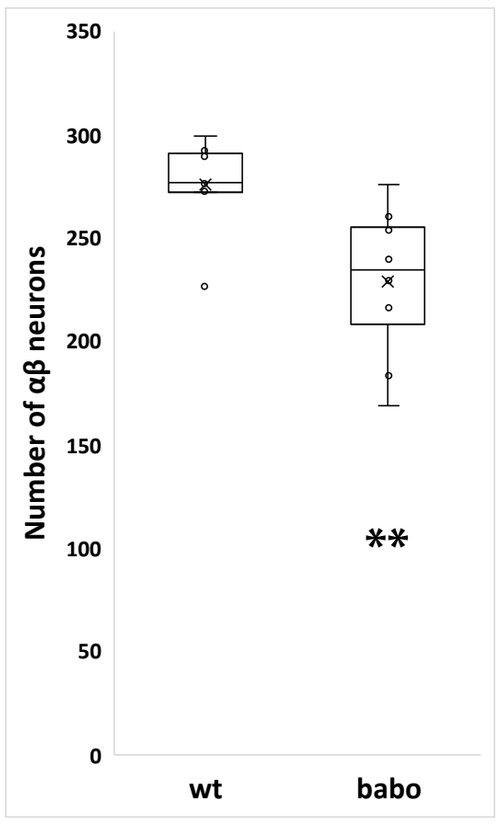

# Wandering L3: *mb-Gal4* MARCM neuroblast clones induced at L1

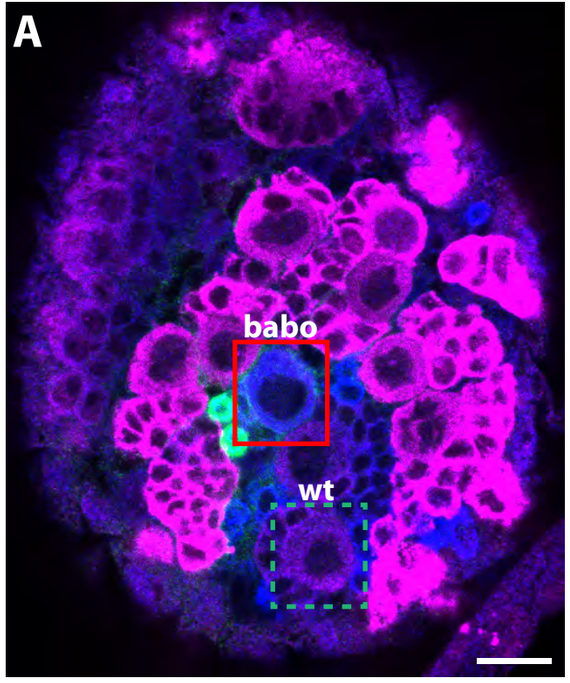


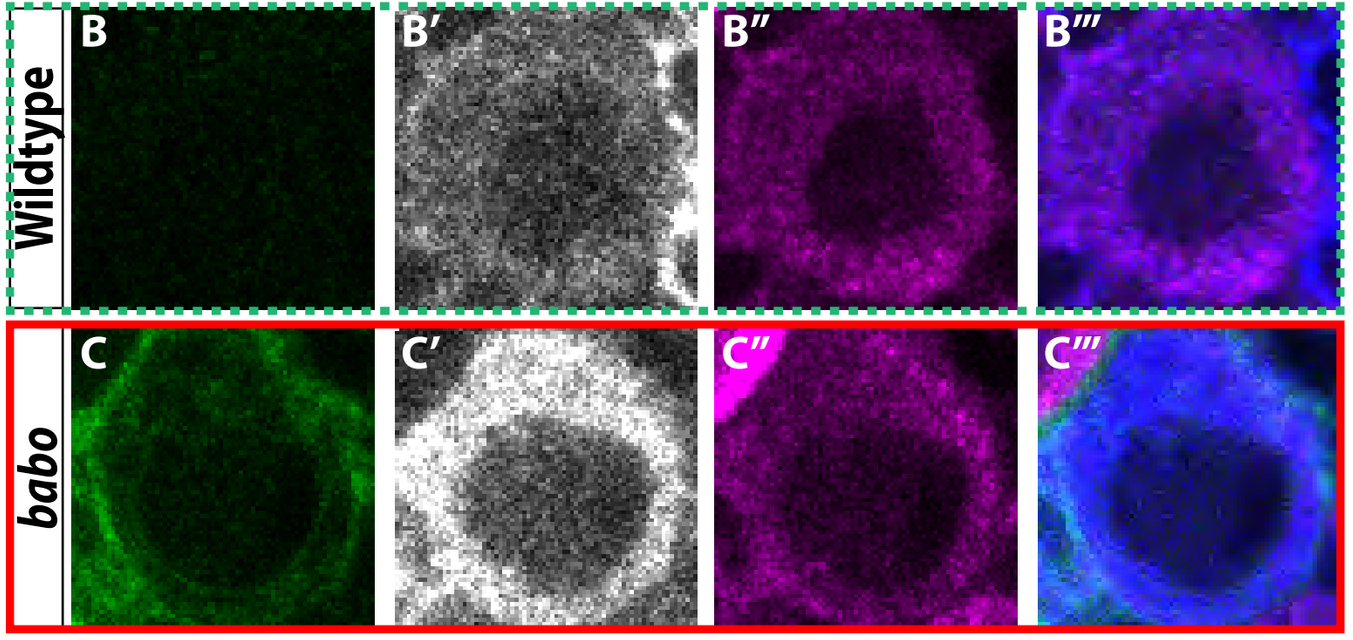


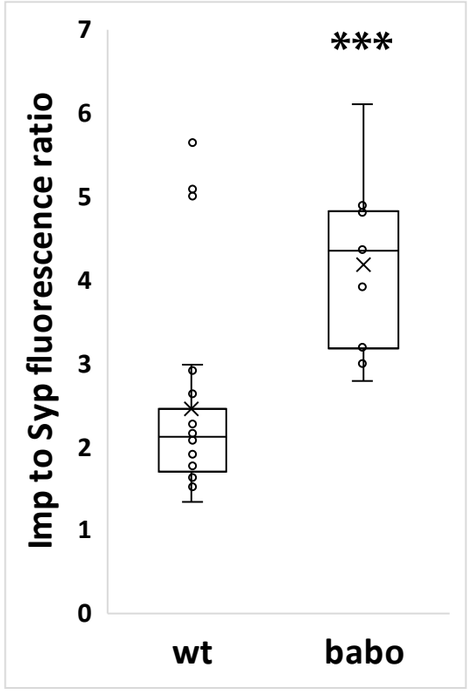

## Adult: *mb-Gal4* MARCM neuroblast clones induced at L1

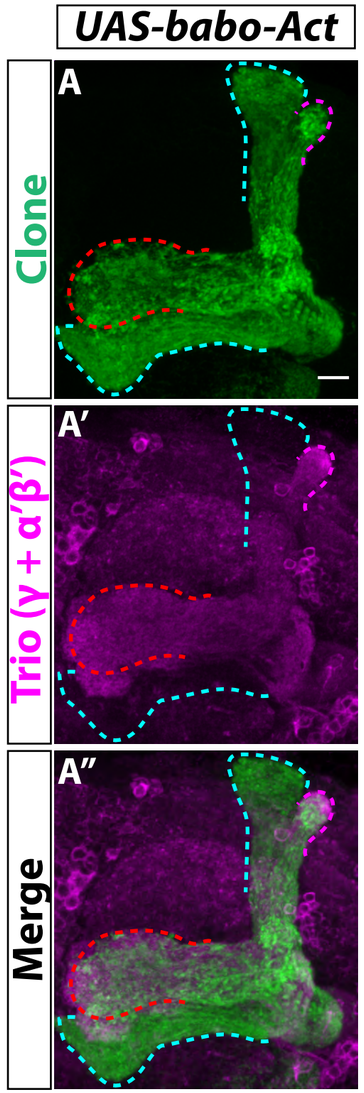


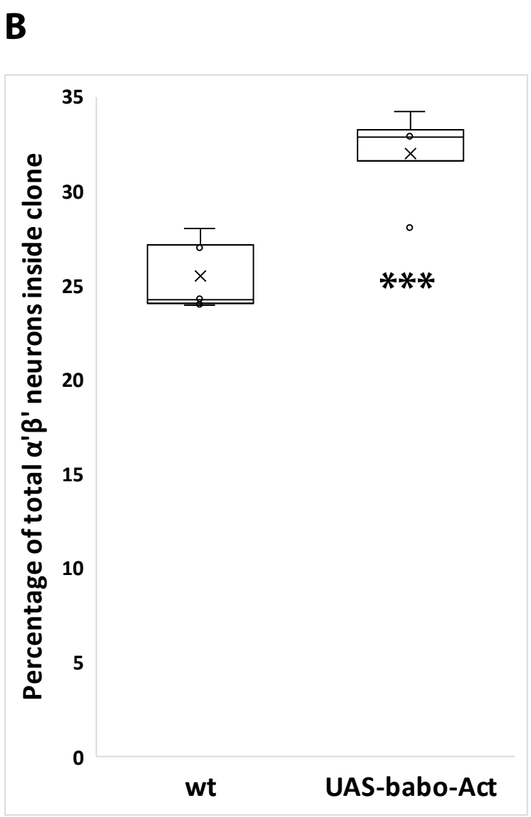


## Wandering L3: *mb-Gal4* MARCM neuroblast clone induced at L1

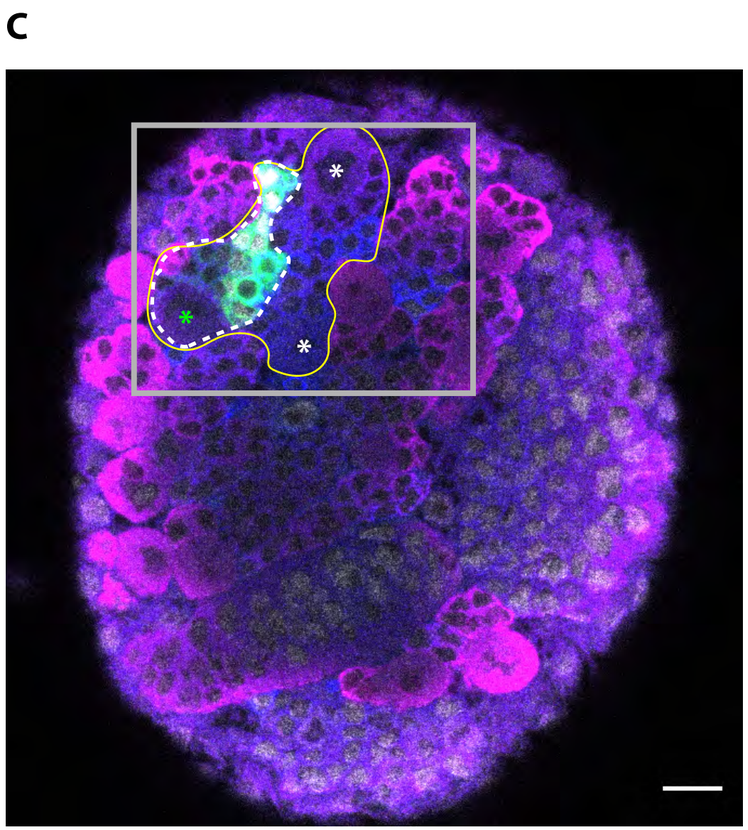


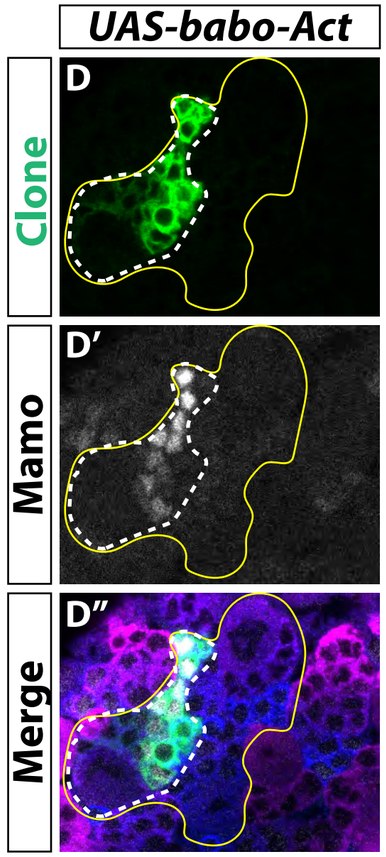

## Adult axon region: *repo-Gal4*

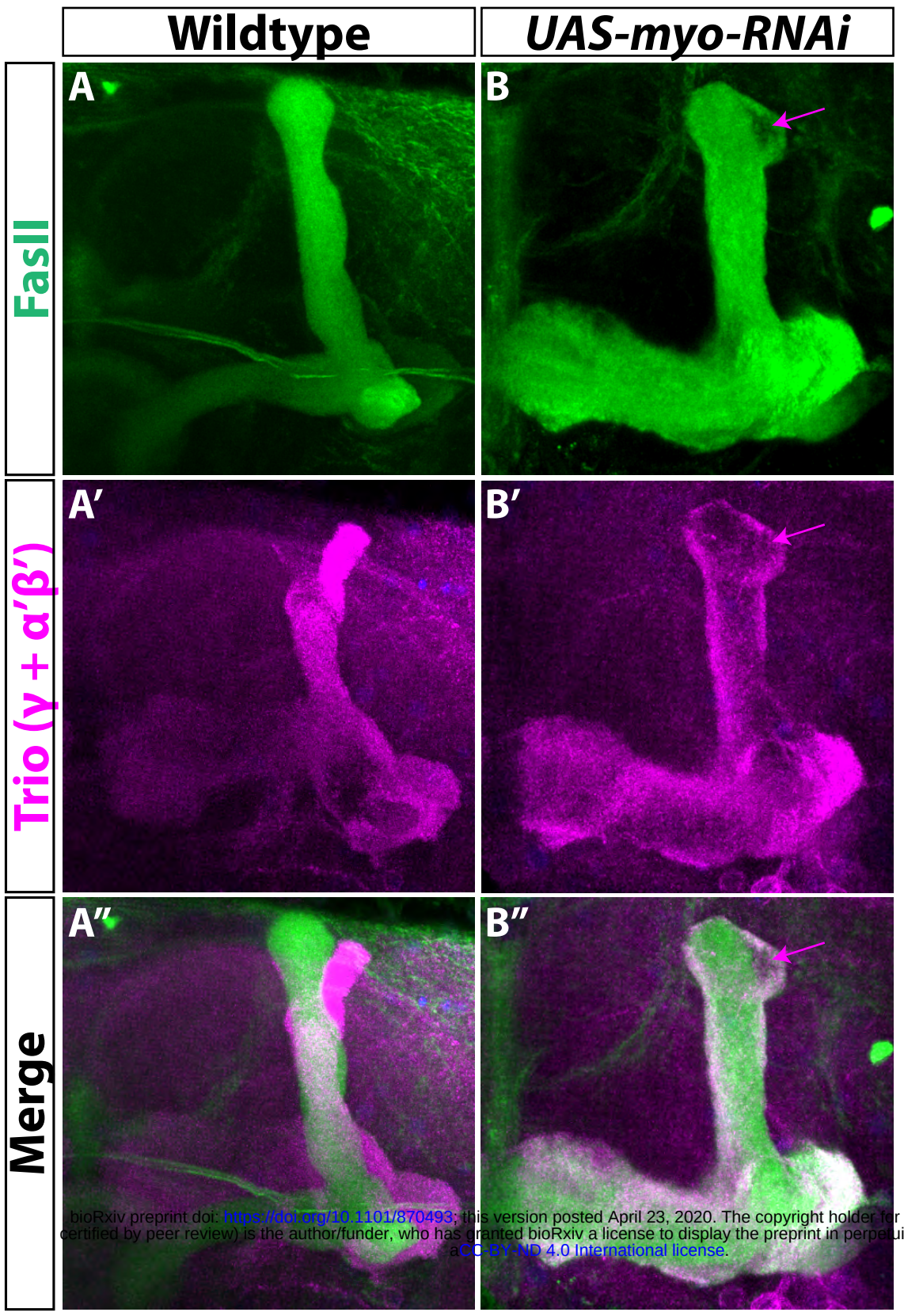




## Adult axonal morphology: γ, α′β′, αβ

## Adult cell body region: *repo-Gal4*

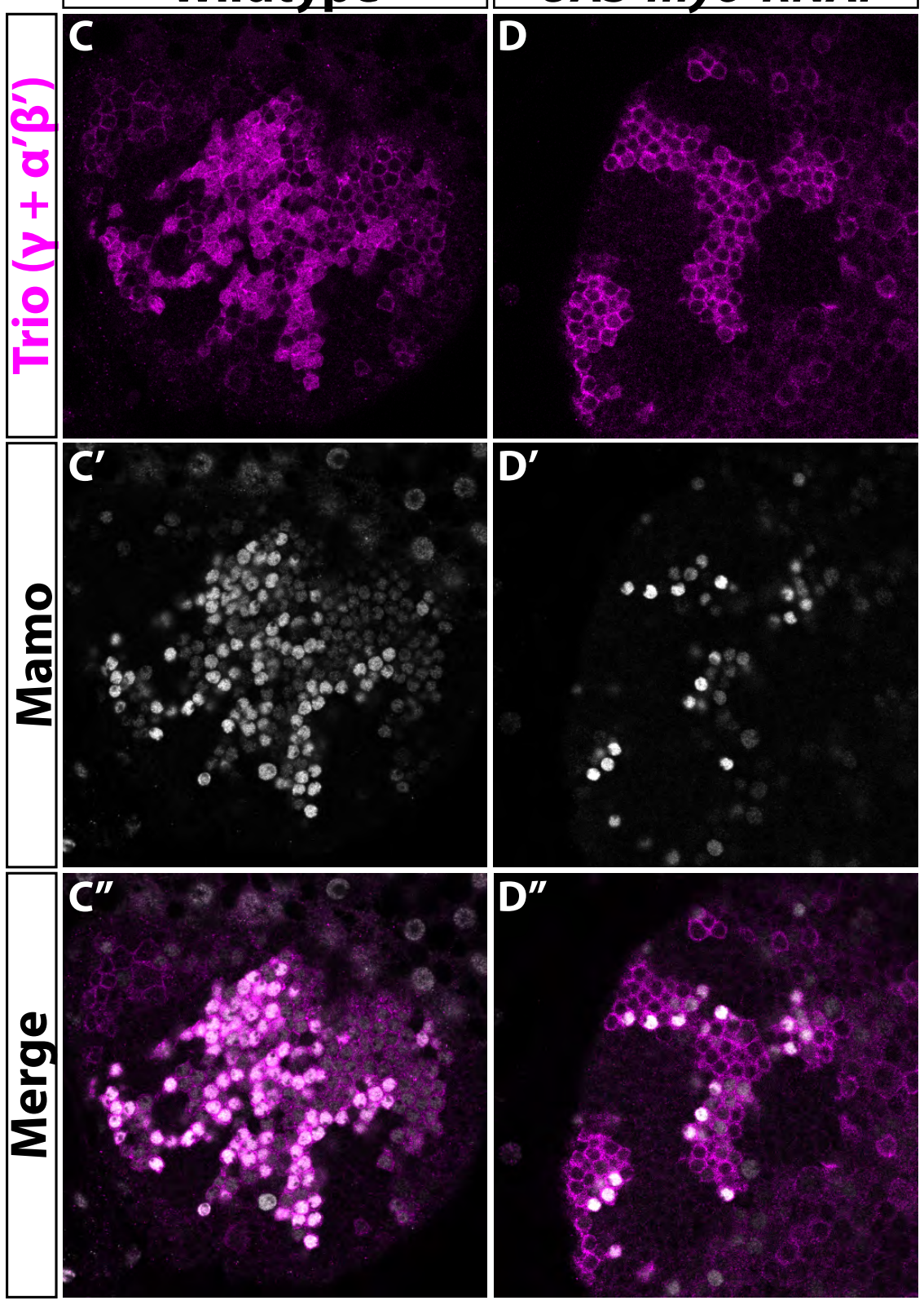


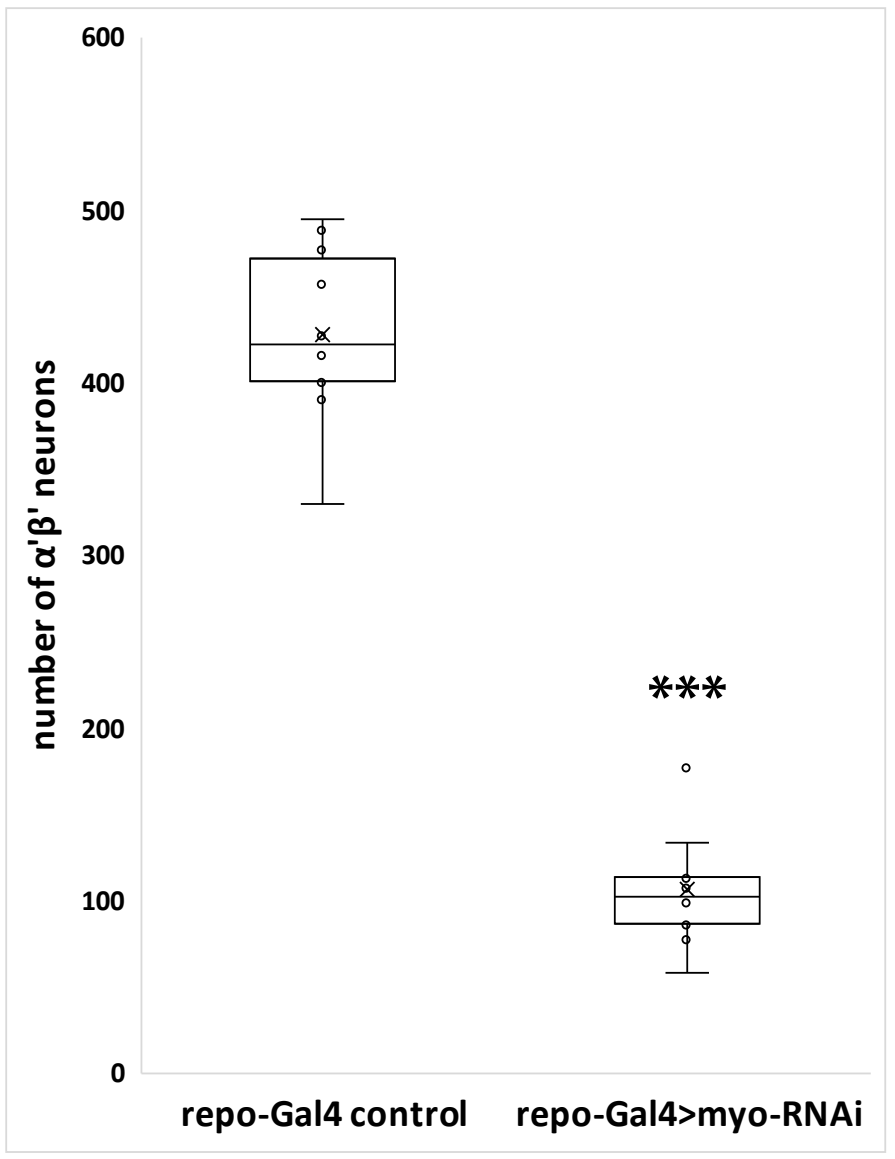


## Wandering L3: *repo-Gal4*

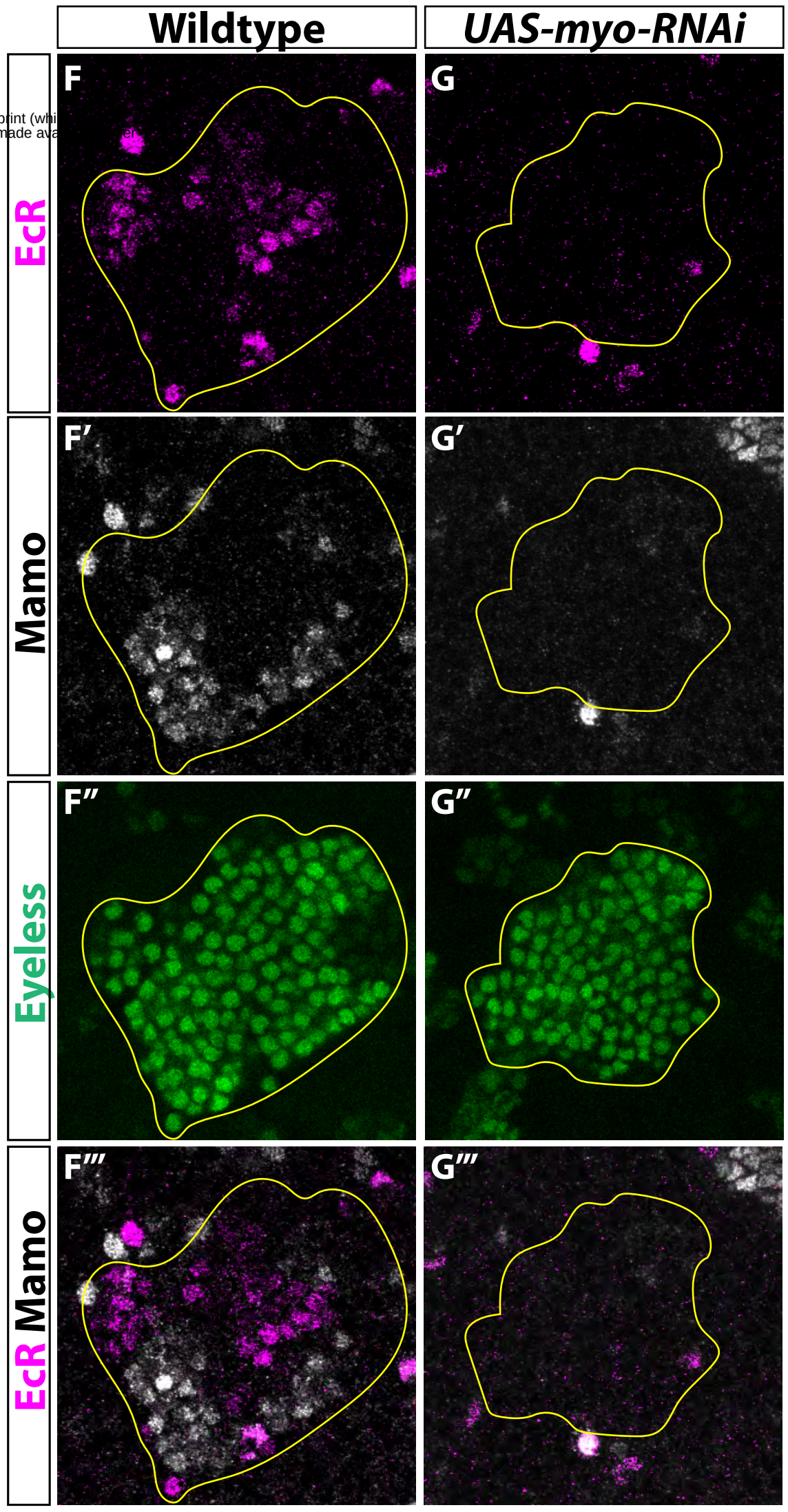

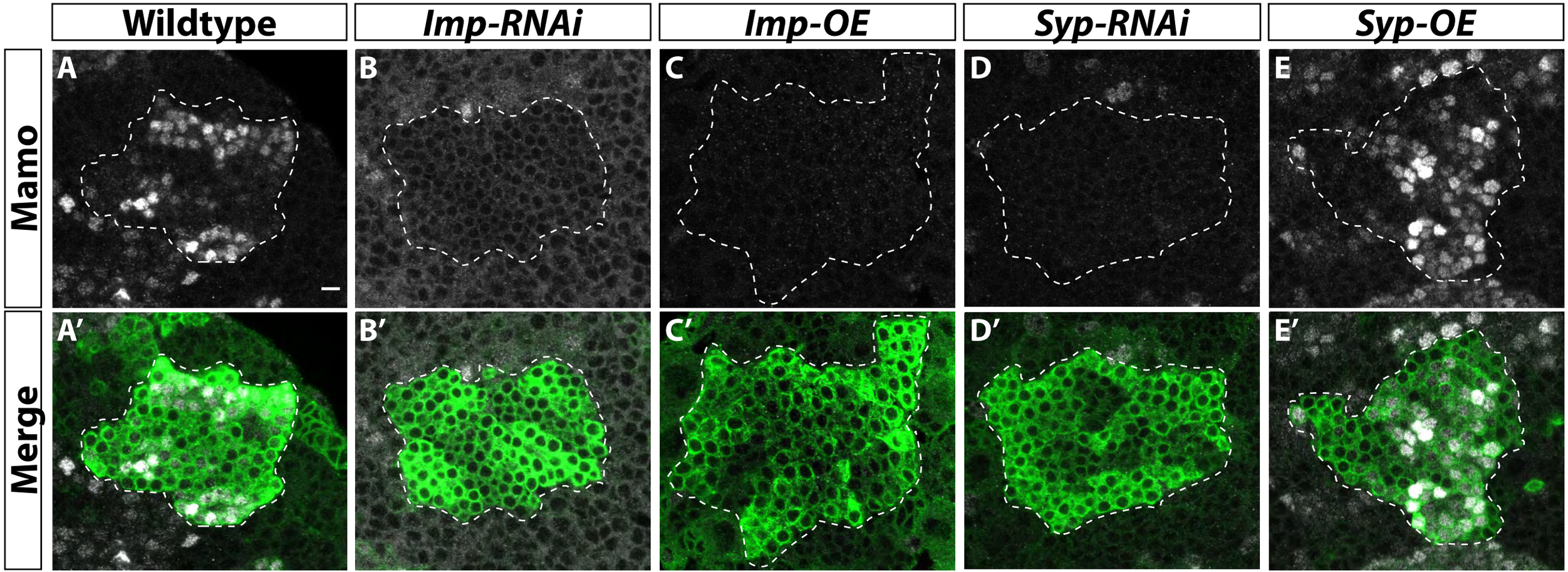
Wandering L3: mb-Gal4
Wildtype
Imp-RNAi
Imp-OE
Syp-RNAi
Syp-OE
Mamo
Merge
A
B
C
D
E
A'
B'
C'
D'
E'

## Adult: *mb-Gal4* MARCM neuroblast clones induced at L1

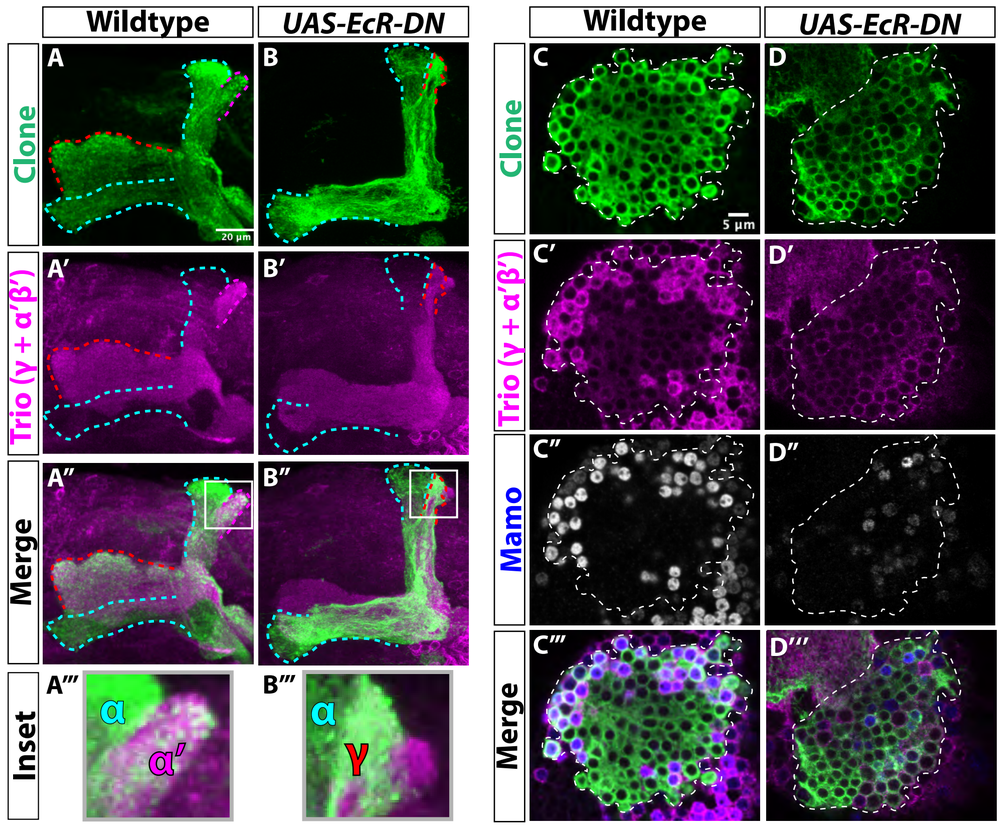


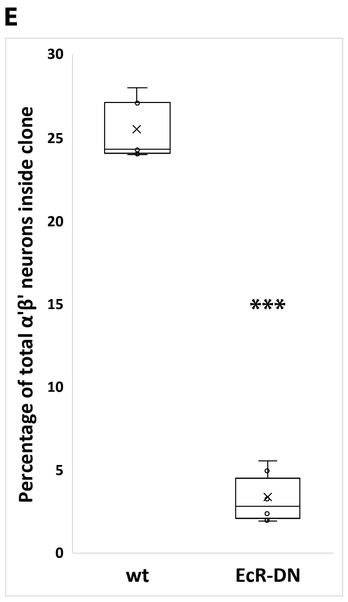


## Wandering L3: *mb-Gal4* MARCM neuroblast clones induced at L1

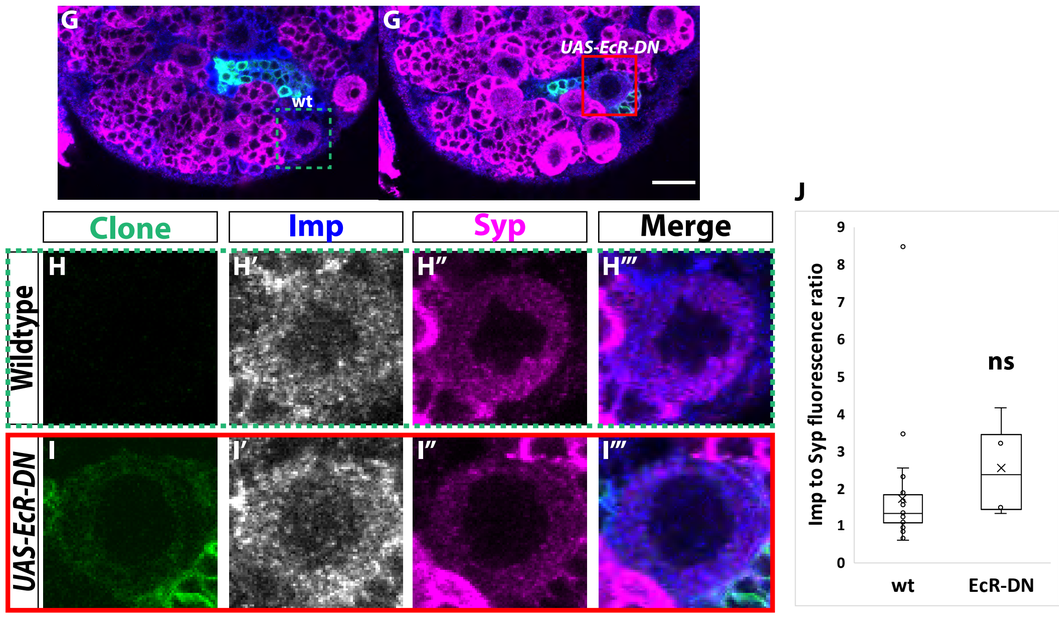


## Adult: MARCM neuroblast clones induced at L1

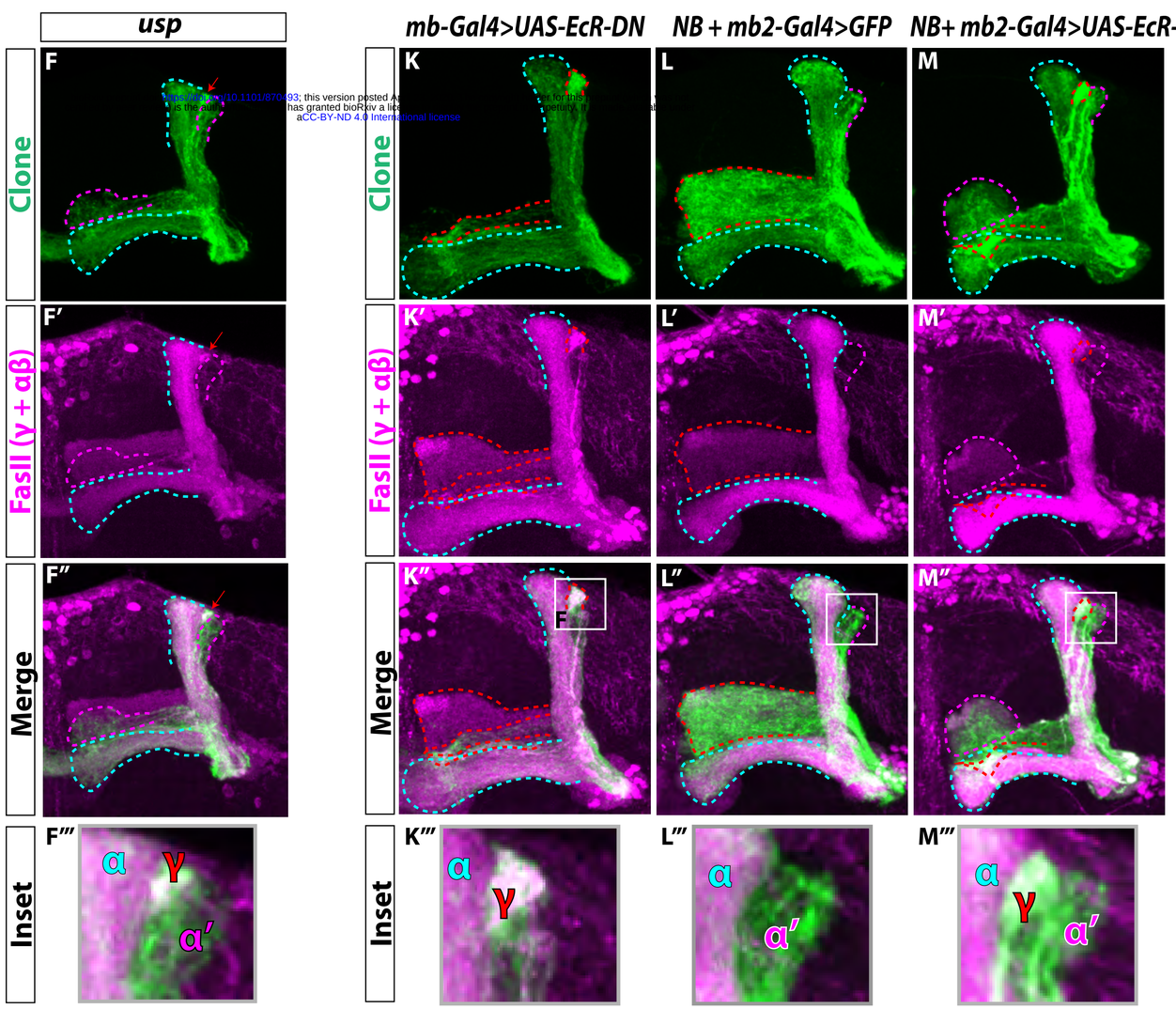




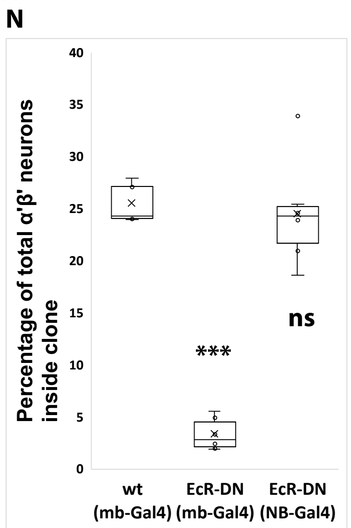


## Wandering L3: *mb-Gal4*

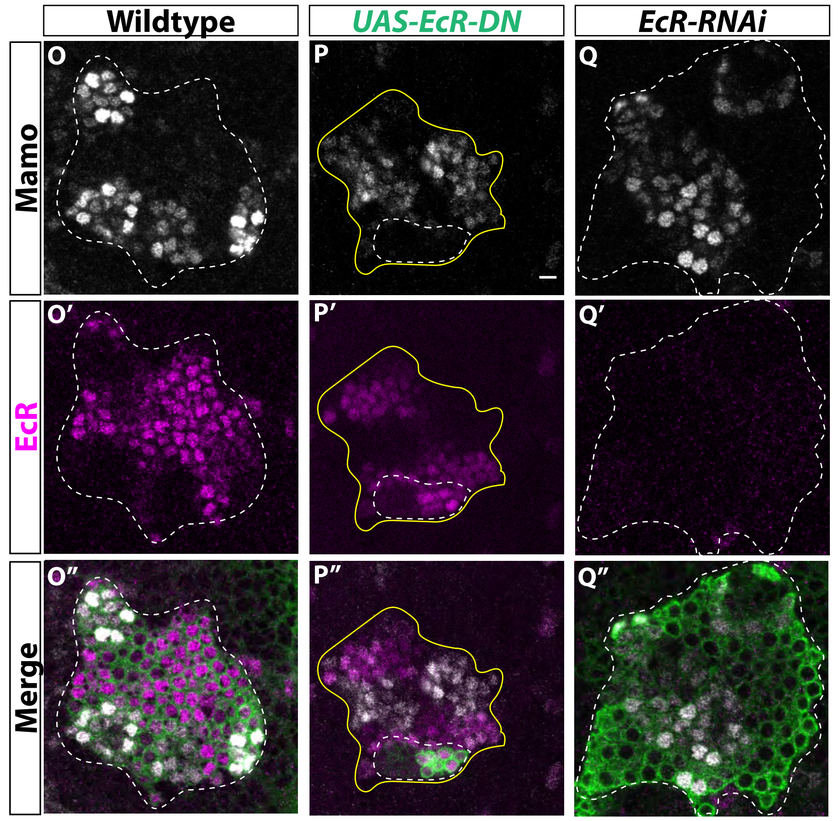


**Adult axonal morphology: γ, α′β′, αβ**

**Adult axonal morphology: γ, α′β′, αβ**

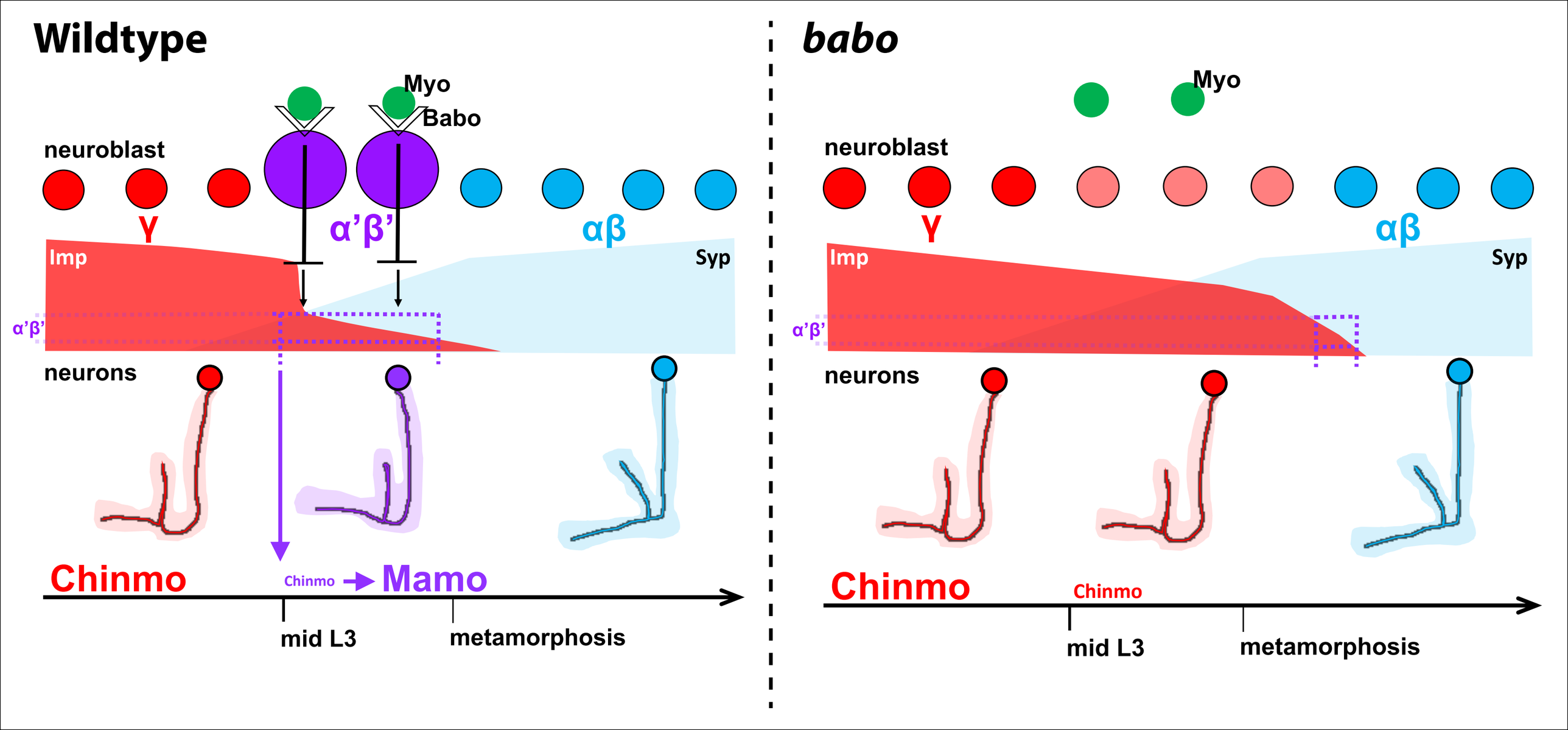
Wildtype
Myo
Babo
neuroblast
γ
α'β'
αβ
Imp
Syp
α'β'
neurons
Chinmo
Chinmo → Mamo
mid L3
metamorphosis
babo
Myo
neuroblast
γ
αβ
Imp
Syp
α'β'
neurons
Chinmo
Chinmo
mid L3
metamorphosis